Mathematics in Bioscience
(Master's Program)

Technische Universität München

Master's Thesis

Exploring the Anti-Cancer Drug Resistance via an agent-based hybrid model

Author:	Olga Khrutska
Examiner:	Prof. Dr. Christina Kuttler
Advisor:	Dr. Judith Pérez-Velázquez
Thesis handed in on:	September 15, 2015

I hereby declare that this thesis is my own work and that no other sources have been used except those clearly indicated and referenced.

September 15, 2015 Olga Khrutska

Abstract

Cancer resistance is one of the major issues arising during chemotherapy, reducing drug efficacy and adversely affecting treatment outcome. One of the main factors allowing cancer cells to acquire anti-cancer drug resistance is exposure to the medication itself.
Gevertz et al. approached this problem in [9], by creating a hybrid discrete-continuous mathematical model to describe the behavior of cancer cell population and the arising of drug resistance when treated with the continuously administrated DNA damaging drug. The purpose of this thesis is to extend the aforementioned study by introducing different drug administration protocols into the model and to investigate the impact they have on the spatial and temporal cancer population dynamics, its clonal diversity and emergence of anti-cancer drug resistance.
Using a piecewise constant function drug scheduling was modeled by diving the total treatment time into equal-length fractions of active drug delivery and resting intervals. Additionally the dose-response curves were presented to analyze the drug potency for different resistance types.
Careful analysis of simulations results revealed that application of drug administration protocols with no-drug intervals will benefit patient's condition by decreasing the overall toxicity burden compared to the continuous drug supply. However, if cancer cells population is not eradicated completely paused drug delivery will lead to increased tumor heterogeneity, creating further complications for the treatment. Moreover, the schedules with low drug dose intensity will surely enough lead to the disease progression and thus, its usage should be avoided.
The obtained results contribute to the future research when modeling specific treatment protocols.

Zusammenfassung

Die Krebsresistenz ist eines der wesentlichen Probleme, die bei der Chemotherapie auftaucht. Sie reduziert die Wirksamkeit der Medikamente und benachteiligt das Behandlungsergebnis. Einer der wichtigsten Faktoren der die Krebszellen ermöglicht die Anti-Krebs-Medikamentenresistenz zu erwerben, ist der Kontakt mit dem Arzneimittel selbst.
Gevertz et al. setzten sich mit dieser Problematik in [9] auseinander, indem sie ein hybrides diskret-kontinuierliches mathematisches Modell erstellten um das Verhalten der Krebszellenpopulation und die Entstehung der Medikamentenresistenz bei Behandlung von fortlaufend ausgeführten, DNA zerstörenden Medikamenten zu beschreiben.
Die Zielsetzung dieser Masterarbeit ist es, die obengenannte Forschung auszuweiten indem man unterschiedliche Therapieschemen in das Modell hinein vorstellt. Darüber hinaus die Auswirkung zu untersuchen, die sie auf die räumliche und zeitliche Dynamik von Krebszellpopulation, ihrer klonalen Vielfalt haben und die Entstehung der Anti-Krebs-Medikamentenresistenz zu erforschen.
Stückweise konstante Funktionen verwendend wurde eine Medikamentenlieferungsplanung erstellt, indem die ganze Behandlungszeit in gleich lange Phasen von aktiver Medikamentenverabreichung und Ruheintervall getaucht wurde. Zusätzlich wurden die Dosis-Wirkungs-Kurven präsentiert um die Medikamentenwirksamkeit von verschiedenen Resistenztypen zu analysieren.
Die sorgfältige Auswertung der Simulationsergebnisse machte deutlich, dass die Anwendung von Therapieschemen mit den Intervallen ohne Medikamentenzufuhr positive Auswirkungen auf die Verfassung des Patienten bei Verminderung der gesamten Toxizität Belastung hat, im Vergleich zur kontinuierlichen Medikamentenverabreichung. Doch wenn die Population der Krebszellen nicht komplett ausgerottet wird, wird die pausierte Medikamentenzufuhr zu einer Steigerung der Tumorheterogenität führen, die weitere Komplikationen der Behandlung erzeugt. Zudem werden die Pläne mit niedriger Intensität der Medikamentendosis mit Sicherheit zum Fortschritt der Krankheit führen und daher sollte die Behandlung vermieden werden.
Die erzielten Ergebnisse trägt zur zukünftigen Forschung bei wenn spezifische Therapieschemen entwickelt werden.

Acknowledgments

I would like to extend my utmost gratitude to my advisor Dr. Judith Pérez-Velázquez from Helmholtz Zentrum München for her guidance, encouragement and continuous support through the course of this work. She is an amazing and wonderful person, possessing an immense knowledge of her field and is always willing to help anyone who asks for it.
I would also like to thank Prof. Kasia Rejniak from H. Lee Moffitt Cancer Center and Research Institute for her brilliant ideas and thoughtful scientific advices.
Special thanks to Prof. Christina Kuttler for being a source of inspiration and motivation during my university years, as I feel fortunate and blessed for the opportunity to take her interesting classes.
And I am also very grateful to my family and my wonderful friends, who were always there for me, cheering me up and supporting me all the way through this thesis.

Contents

List of Figures

List of Tables

1 Introduction

Chemotherapy, being one of the conventional cancer treatment options, might be used as first-line cancer therapy, neoadjuvant or adjuvant treatment as well as be combined with other therapeutic modalities, depending on the malignancy type, stage and patient's health condition. Since, traditionally used anti-cancer drugs are cytotoxic, chemotherapy is usually accompanied by their negative side effects. Therefore, while planning treatment protocols no-drug intervals must be introduced between active administration of the medication to grant normal cells time to recover. However, also the remaining tumor cells will proliferate during the resting intervals which may further lead to the therapy failure[20]. Another issue that adversely affects treatment success is tumor resistance. Anti-cancer drug resistance might exist prior to the treatment course or might be induced by medication use as well as by the cell interaction with microenvironment or other conditions (acquired resistance)[45, 50, 49].
A hybrid discrete-continuous model describing a tumor, growing in the small tissue slice, supplied with oxygen from the vasculature and treated with DNA damaging drug, was presented in [9, Gevertz et al. 2015]. The model regards oxygen and drug concentrations as continuous variables determining their dynamics through reaction-diffusion equations. Tumor is described using agent-based approach, with a particle-spring system depicting cancer cells as particles with assigned elastic springs generating forces whenever displaced from the equilibrium. The characteristics of the model enable the monitoring of each cell separately, thus, revealing its individual properties and cell life history. However, [9, Gevertz et al. 2015] assume constant drug supply throughout the treatment course what differ from clinical practice. Thus in continuation to the presented analysis of numerical simulations for the stated model this thesis incorporates the idea of resting intervals, dividing the whole treatment time into fractions and alternating active drug therapy with no-drug periods.
Chemotherapy protocols are tumor-specific and designed taking into consideration patient's health condition and cancer response to the treatment. Medical doctors prepare chemotherapy plans for patients according to the existing practice guidelines and clinical trials. Depending on cancer type they select an appropriate schedule, with specified duration, frequency and number of drug administration cycles. However, in this thesis a simplifying assumption was made by considering a generalized chemotherapy regimen with equal-length intervals and fixed dose intensities in active drug administration periods. Tumor cell population behavior treated with pulsed drug supply is compared with the ones that receive medication continuously. Further, the modifications of drug dose intensity for some protocols were provided in order to adjust the schedule to the tumor response as it is frequently done in the clinical practice.
Chemotherapeutic agents considered in the thesis are DNA damaging drugs including

alkylating agents, platinum-based anti-cancer drugs, antimetabolites, anthracyclines and topoisomerase poisons. The exposure to DNA damaging drugs induces drug resistance in cancer cells, as some mid-repaired lesions will be replicated, due to the increased DNA damage tolerance, thus, potentially accumulating mutations [37, 4]. Chemotherapeutic agents are traditionally considered to be the most effective at high concentrations, however, due to the narrow therapeutic window, the unwanted drug side-effects are inevitable. Thus, conventional chemotherapy regimens delivering cytotoxic drug at maximum tolerated dose are accompanied by a high toxic burden for a patient. Dose-response plots, provided in this thesis, give insight into medication's characteristics suggesting reasonable drug dosages for the treatment.
As mentioned before, anti-cancer drug resistance is a great obstacle in the way of successful treatment outcome, decreasing the effect of anti-cancer drugs [3, 7, 51]. This thesis focuses on the secondary resistance neglecting the pre-existing one as to simplify the analysis of model's numerical simulations. Conditions that might trigger drug resistance remain of particular scientific interest [6, 36, 5, 13, 48, 11], however, the analysis targets mainly micronvironment and drug exposure.
Human cancers are heterogeneous by their nature, differing not only between patients but also within a single cancer site (intratumoral heterogeneity)[2].Treatment of heterogeneous tumors is much more complex compared to the homogeneous ones as only some of the clones respond to the drug. Moreover they are considered to be yet another cause of anti-cancer drug resistance [23, 21, 25]. Failed treatment is inevitably followed by the resistant clones' expansion after drug administration, due to "selective pressure" enforced on cancer cell population by drug exposure [10, 30]. Therefore, this thesis examines, inter alia, tumor clonal evolution induced by the different drug administration schedules.
A comparison of the different drug administrating regimens under the same initial conditions was presented in this thesis. The results obtained from numerical simulations analysis revealed that disease development for all tumor resistance types is indeed affected by the choice of particular treatment protocol, showing distinct behavioral patterns depending on dose intensity and number of fractions.

2 Literature Review

2.1 Cancer Biology

2.1.1 Cancer definition

Presently cancer is the most common disease all over the world, affecting people of all ethnic and racial groups, social classes and age. Although cancer researchers worldwide are investigating new treatment methods and improving the existing ones, cancer remains one of the leading morbidity and mortality causes [12]. According to [43] there were around 14.1 million of new cancer cases and 8.2 million cancer deaths registered in 2012 and these numbers are expected to increase in following years owing to "growth and aging of the world population".
The origin of the word cancer is attributed to the terms carcinos and carcinoma used by Hippocrates (460-370 BC) to describe non-ulcer- and ulcer-forming tumors because of their resemblance to a crab although it is known that human beings suffered from it long time before [42]. Thus some of the earliest evidences of bone cancer were found in the mummies from ancient Egypt and there are cases reported ancient manuscripts (1600 BC)[1]. Cancers are a broad range of diseases manifesting in a similar clinical picture of a cell group in an uncontrolled division which ultimately invades neighboring tissues and causes systematic breakdown of the whole organism [22]. Being a disease of chaotic disruption in nature, cancers are sometimes ironically referred to as an universal way of dying should the organism manage to live long enough. The vulnerability to cancers is inherent to all multicellular life and in order to gain insight into what gives rise to cancer it is necessary to outline the basic principles of organism development.

2.1.2 Cell cycle and multicellular ontogenesis

Most multicellular organisms are made up from cells having the identical genetic material. As the need of cell replacement arises, cells divide and specialize into distinct types in order to accomplish a certain predefined function. This process is tightly regulated by the interaction between cell's genetic material and organisms signalling pathways or other means to influence cell fate. Although some taxa evolved to have their specialized cells discard the portion of genetic material they don't directly need thus ensuring irreversibility of specialization process, such practice is relatively uncommon. Generally, the cells retain all of the genome, but have an elaborate biochemical reaction network that is used to switch certain parts on and off during the normal cell operation [39].
Not only the specialization is thus regulated, but the very division itself can not be allowed to occur at random lest the cell and tissue state is thrown out of balance. Cells in

an organism undergo a special division *cell cycle* (Figure 2.1) and, unlike bacteria and

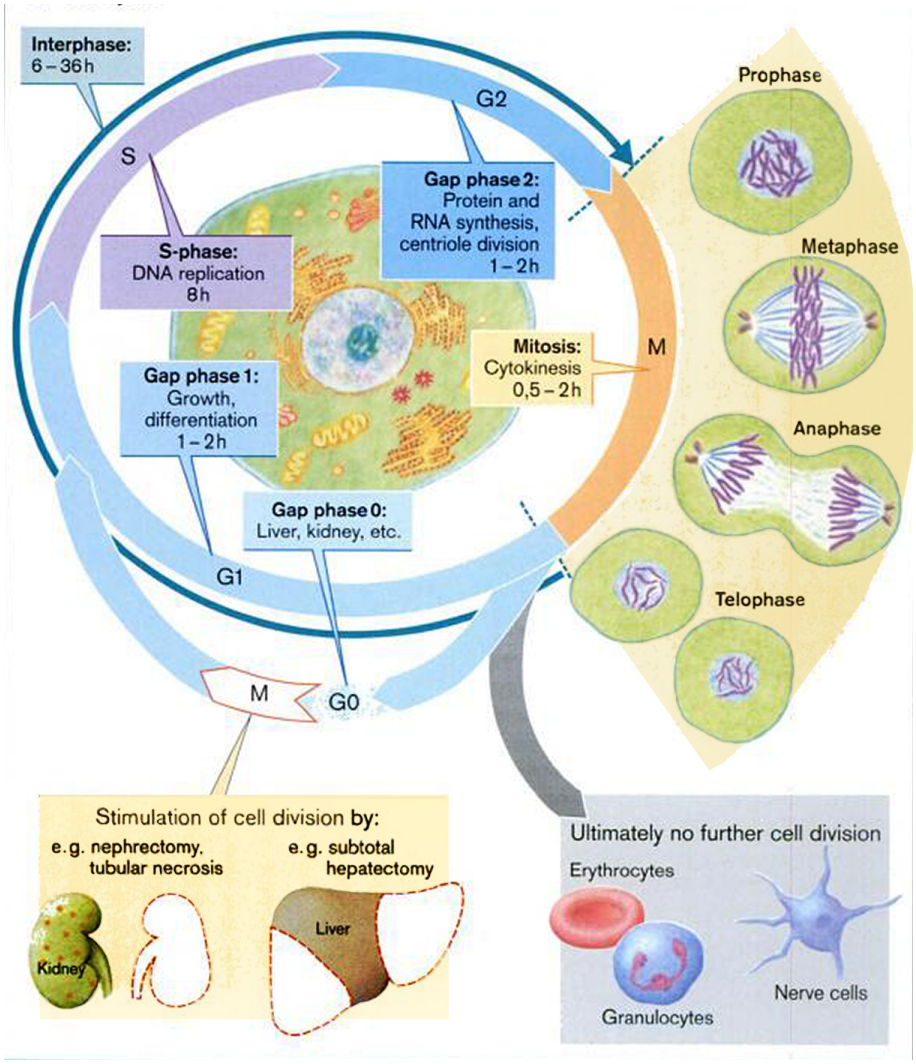

Figure 2.1: *Cell Cycle* [40, Color Atlas of Pathophysiology]

unicellulars, the process is not continuous, but instead has points in which the cell is *restricted* and is forced into a certain state until allowed to go further. In addition to cell birth, the death of existing cells is also programmed. As a stage of division, the cell has to replicate its DNA, a process that is known to be erroneous producing errors called *mutations*. Should the cell detect an inconsistency whilst copying the genome, it either attempts to fix the mistake by proofreading mechanism, or aborts the division altogether usually resulting in dividing cell dying. Not only the cell itself can initiate the self destruction process, but a normally functioning cell can also be induced to do so by immune system, which is crucial for early stage cancer prevention. This ensures a hight cell turnover, a typical human body contains about 10^{13} cells at the time while

the total amount of the individual cells formed during the lifetime on average is as high as 10^{16} [39].
Sometimes, as a result of the regulatory disruption or mutations, groups cells tend to break away from the regulatory processes and start functioning with varying degrees of autonomy. This means that such malfunctioning cells in general ignore the self-destruction command coming from the organism and typically reproduce quite quickly in their own rhythm without any stimulation for doing so. A practical result of such malfunction manifests in a *tumor*, which is a collection of uncontrollably dividing cells. Formally not all tumors are leading to cancer as a disease, in some cases the control over the cells is only partially broken and the tumor is called *benign*. Such tumors are easily operable most of the time and lack the invasive abilities, therefore staying localized. *Malignant* tumors in contrast have the ability to invade neighboring tissues and produce secondary tumors called *metastasis*. Such tumors are what is generally considered to be cancer, and metastasis are the factor that causes body damage and most likely death [33].
As the organism complexity increases, the regulatory networks tend to grow overloaded and fragile. As the result, more advanced populations in general have bigger risks of cancer, compared to less developed ones. In particular, while invertebrate tumors have been reported, it is noted that those are seldom cancerous. Furthermore, invertebrates have strikingly lesser rate of virally-induced tumor formation even compared to other species of the same habitat. There is an opinion that the vertebrate adaptive immune system offered an additional selective pressure that ultimately gave rise to the deadlier malignant tumors which were able to escape its action [17].

2.1.3 Causes of cancer

Typically cancers arise from a prolonged contact with the specific class of agents called *carcinogens* for this property. While the events of tumor appearance are random in nature and constantly occur in normal body state, it is the carcinogen overexposure that makes them statistically more likely to develop into actual cancers. While some of carcinogenic chemicals such as tobacco smoke, alcohol, various tars and soot are well known, carcinogens are surprisingly widespread in nature and typical human environment [47]. Many cooking methods in particular give rise to carcinogenic species although many raw foods counter-intuitively also are an abundant source of compounds that are able to cause cancers.
Virtually all substances that are known to induce genetic mutations have shown to cause cancers. The reverse is not true however, as there are verified carcinogens that posses no observable mutagenic activity whatsoever. It is thought that those compounds interact with the cell metabolic network without directly influencing the cell's genetic material itself. A carcinogen is not bound to be a chemical compound, physical effect of environment are also able to share the carcinogenic effect. A classical example of a non-chemical carcinogenic effect is the radiation, including sunlight. It was also

shown that certain bacteria may also be responsible for tumor formation, as such many stomach cancers are linked to *Helicobacter pylori* bacterium which infects the stomach walls mucous layer. Virii [22] also present another substantial cause or at least a facilitation factor for cancers development attributed to as high as 15% of cases worldwide. Despite the relative abundance, viral cancers can be potentially treated more easily due to the ability to distinguish between normal and infected cells on the basis of viral genetic and protein material presence [18].
Different cancer types are spread unequally across the world. While some have no direct cause associated with them and occur at the comparable rate in most human populations, others show regional or ethnic specificity. Hereditary predisposition can explain some of cancers, although it is not uncommon for the migrant populations to have a wastly different cancer statistics than those of the home population hinting at the fact that the lifestyle and the environment indeed is also a substantial factor [33].

2.1.4 Classification of cancers

Cancers can be classified by the location in the body where tumor originated or by the tissue from which it developed (histological type). There are four major groups of cancers from histological point of view:

- Carcinomas
- Sarcomas
- Hematopoietic malignancies
- Neuroectodermal malignancies

Carcinomas are the most common human cancers and they have epithelial origin. There are two major groups of carcimonas:

- Squamous cell carcinomas - tumors that originate from epithelial cells forming protective cell layers. They appear on skin, in lungs, nasal cavity, oropharynx, larynx, esophagus, cervix.
- Adenocarcinomas - tumors that originate from duct or cavity lining substance secreting cells the ducts or cavities. This carcinomas arise in lungs, breast, stomach, pancreas, esophagus, colon, prostate, endometrium, ovary.

Sarcomas origin from the connective tissues of mesenchymal cell types. Commonly they can develop from the cells that are forming bones (osteoblasts), fat cells (adipocytes), smooth and striated muscle cells, connective tissue cells (fibroblasts), cells that lean blood vessels (endothelial cells) and cells that form cartilages (chondrocytes).
Hematopoietic malignancies represent the group of other nonephitelial cancers that originate from blood-forming tissues. This group includes leukemias, lymphomas and myelomas.

Neuroectodermal malignancies (glioblastoma, astrocytoma, meningiomas, schwannoma, retinoblastoma, neuroblastoma, ependymoma, oligodendroglioma, medulloblastoma) arise in the tissues that originated from the outer cell layer of the early embryo [33]. Malignant tumors' histological classification and clinical description plays significant role in the treatment planning, prognosis, estimation of the treatment results, information exchange between medical centers and in future research. Classification approach in medical practice is particularly based on subdivision of tumors by the stage of their development. The Classification of Malignant Tumors (TNM) [41] is developed to harmonize the presentation of clinical data. The TNM consists of three main components which are accompanied by numbers which indicate the degree of incidence:

- T (tumor) - expansion of the primary tumor
- N (nodes) - presence or absence of the metastases in regional lymph nodes and the degree of their damage
- M (metastases) - presence or absence of the remote metastases

This kind of classification gives a pretty accurate description of the tumor's anatomic distribution.

2.1.5 Diagnostics

Nowadays cancer is a one of the major health problems in the world and the treatment efficiency mostly depends on its early detection and diagnosis. Cancer screening is used to detect cancer on predominantly healthy persons who have no symptoms of the disease [16]. The methods of screening are different depending on a cancer type and usually they are age-dependent. Among them the most effective in the terms of death reduction are mammogram (the x-ray breast examination) for the breast cancer [27], Pap test (detection of the cell changes on the cervix) and HPV test (detection of human pappilomavirus, which is known to cause changes of the cervix cells) for the cervical cancer [28], low-dose helical computed tomography for lung cancer, colonoscopy, sigmoidoscopy and high-sensitivity fecal occult blood tests (FOBTs) were shown to reduce deaths from colorectal cancer [15].
Usually cancer is diagnosed using cells (cytology or cytopathology) or tissue samples (biopsy). In the most cases it is enough to proceed microscopic examination of collected samples for abnormalities (like size and shape of cells and their nucleus, arrangement of the cells etc.) to detect the cancer, its type and to grade it, but in some situations there is a necessity to perform a specific test for proper diagnosis (histochemical and immunohistochemical stains, electron microscopy, flow and image cytometry, various genetic tests) [44].

2.2 Chemotherapy

2.2.1 History of chemotherapy

The use of chemotherapy to treat cancer began at the start of the 20th century with attempts to narrow the universe of chemicals that might affect the disease by developing methods to screen chemicals using transplantable tumors in rodents. In the early 1900s, the famous German chemist Paul Ehrlich set about developing drugs to treat infectious diseases. He was the one who coined the term "chemotherapy" and defined it as the use of chemicals to treat disease. He was also the first person to document the effectiveness of animal models to screen a series of chemicals for their potential activity against diseases, an accomplishment that had major ramifications for cancer drug development. In 1908, his use of the rabbit model for syphilis led to the development of arsenicals to treat this disease. Ehrlich was also interested in drugs to treat cancer, including aniline dyes and the first primitive alkylating agents, but apparently was not optimistic about the chance for success [8].
Surgery and radiotherapy dominated the field of cancer therapy into the 1960s until it became clear that cure rates after ever more radical local treatments had plateaued at about 33% due to the presence of heretofore-unappreciated micrometastases and new data showed that combination chemotherapy could cure patients with various advanced cancers. The latter observation opened up the opportunity to apply drugs in conjunction with surgery and/or radiation treatments to deal with the issue of micrometastases, initially in breast cancer patients, and the field of adjuvant chemotherapy was born. It was four World War II-related programs, and the effects of drugs that evolved from them, that provided the impetus to establish in 1955 the national drug development effort known as the Cancer Chemotherapy National Service Center. The ability of combination chemotherapy to cure acute childhood leukemia and advanced Hodgkin's disease in the 1960s and early 1970s overcame the prevailing pessimism about the ability of drugs to cure advanced cancers, facilitated the study of adjuvant chemotherapy, and helped foster the national cancer program. Combined modality treatment, the tailoring of each of the three modalities so their antitumor effect could be maximized with minimal toxicity to normal tissues, then became standard clinical practice [35].
Today, chemotherapy has changed as important molecular abnormalities are being used to screen for potential new drugs as well as for targeted treatments.

2.2.2 Cancer treatment

Chemotherapy has three major roles in cancer: as the primary treatment, as an adjuvant to the primary treatment (to prevent or delay relapse), or as palliative therapy to improve symptoms and prolong survival following primary treatment failure. Traditional chemotherapeutic agents are cytotoxic, that is to say they act by killing cells that divide rapidly, one of the main properties of most cancer cells. This means that chemother-

apy also harms cells that divide rapidly under normal circumstances: cells in the bone marrow, digestive tract, and hair follicles. This results in the most common side-effects of chemotherapy: myelosuppression (decreased production of blood cells, hence also immunosuppression), mucositis (inflammation of the lining of the digestive tract), and alopecia (hair loss). Some newer anticancer drugs (for example, various monoclonal antibodies) are not indiscriminately cytotoxic, but rather target proteins that are abnormally expressed in cancer cells and that are essential for their growth. Such treatments are often referred to as targeted therapy (as distinct from classic chemotherapy) and are often used alongside traditional chemotherapeutic agents in antineoplastic treatment regimens. Chemotherapy may use one drug at a time (single-agent chemotherapy) or several drugs at once (combination chemotherapy or polychemotherapy). The combination of chemotherapy and radiotherapy is chemoradiotherapy. Chemotherapy using drugs that convert to cytotoxic activity only upon light exposure is called photochemotherapy or photodynamic therapy [31].
The application of chemotherapy to different types of cancer has different efficiency. Some rare neurological conditions such as primary CNS lymphoma, germ cell tumours, and primitive neuroectodermal tumours are chemo-responsive and chemotherapy plays a central role in their management. However, the majority of brain tumours have been considered chemo-resistant and the use of chemotherapy, particularly as adjuvant treatment, is controversial. With the availability of newer drugs and a better understanding of the biology of brain tumours this situation is changing, even for high grade gliomas. For any chemotherapy agent to be effective it must first penetrate to the cancer and the selective permeability of the blood-brain barrier (BBB) poses a particular problem for brain tumours. Some drugs, because of their small molecular size or high lipid solubility, naturally achieve good BBB penetration (nitrosoureas, temozolomide) and high concentrations in tumour. This can be improved by bypassing the BBB using biodegradable wafers, BBB disruption, or continuous infusion methods. A limited number of drugs, such as methotrexate and cytosine arabinoside, can be given safely by the direct intrathecal route. However, apart from special circumstances, such as childhood acute lymphoblastic leukaemia, they have shown no efficacy in brain tumours [34].

2.2.3 Chemotherapeutic agents - mechanism of action

The following review of chemotherapeutic agents is based on [29].

Alkylating agents

The alkylating agents act by introducing alkylation over the important biopolymers thus inhibiting their normal function. Since DNA is a favored alkylation target, the alkylation drugs depend on cell proliferation for their activity, although they are mostly not cell-cycle-phase-specific. It is possible for th tumors to be resistant against this class

of drugs by enchancing the biopolymer repair mechanisms efficiency thus outperforming the rate at which the damage is caused. Notable classes of alkylating agents include:

Nitrogen mustards Having been developed in the chemotherapeutic capacity after WWII and related toxic gas research [8], such substances as mechlorethamine (Mustargen), cyclophosphamide, isosfamide(Ifex), chlorambucil (Leukeran) are highly active alkylating moiety in aqueous solution, particularly effective against hematopoietic system tumors.

Nitrosoureas Nitrosoureas are very useful for crossing cell membranes thanks to their high lipid solubility. This is particularly important for crossing blood-brain barrier and reach brain tumors. Nitrosoureas act by spontaneously decomposing into chloroethyl diazohydroxide and isocyanate which in turn provide the drug's functional activity.

Platinum agents This class of compounds comprises platinum-containing metal complexes that are able to indroduce inter- and intra-strand DNA cross-links that prevent the biopolymer pathways from functioning.

Antimetabolites

Antimetabolites are analogs of the compounds which are normally involved in cells pathways which have the ability to compete with or substitute their natural counterpart thus resulting in a bogus biopolymer being formed. Because they are most commonly targeting the nuclear acid synthesis pathways, they are most effective during the S phase of the cell cycle during which DNA replication happens and relatively useless against the cell restricted at G_0 phase. Therefore the key target of antimetabolyte drugs are rapidly growing tumors that has a high ratio of cells in active replication. Because the metabolite (and consequently the antimetabolite) uptake is limited by cell metabolic rates, this class of drugs' efficiency is saturated after certain dosage is reached.

Natural substances

Throughout the history, a wide array of naturally ocurring drugs have been documented to have antitumor activity. Some of the important classes of such compounds are presented below:

Antitumor antibiotics Certain antibiotics such as bleomycin (Blenoxane) specifically target DNA at GC/GT sequnces resulting in free radical strand damange and are functional for human cells, therefore enabling their use against tumors. Anthracycline antibiotics produced by *Streptomyces percetus* fungus also have anti-tumor properties, acting both by intercalating the DNA base pairs and inhibiting topoisomerases I and II.

Epipodophyllotoxins Extracted from mandrake (*Podophyllum peltatum*) root, a class of toxins stabilise DNA-topoisomerase complex thus preventing DNA replication and rendering the cell unable to proceed from G_1 phase. Camptothecin analogs which are found in Chinese ornamental tree (*Camptotheca acumiata*) manifest similar action and also are able to interrupt DNA elongation.

Vinca alkaloids The alkaloid compounds foundin periwinkle (*Vinca rosea*) bind the microtubules while the cell is passing the S phase. Their activity becomes apparent only at later M phase when the affected microtubules fail to be recruited and assembled for mitotic spindle formation, therefore rendering the cell unable to complete mitosis.

Taxanes Paclitaxel and docetaxel (Taxotere) are derived from the needles of yew plants (*Taxus baccata*). They attack the similar target as the vinca alkaloids, however instead of disassembling the microtubules, they instead stabilise them locking the cell in the M phase.

3 Agent-based hybrid model

The hybrid discrete-continuous mathematical model, used in this thesis, was developed and presented by Gevertz et al. in [9]. It reconstructs a two-dimensional tissue slice with a cancer cell population located there. The model enables to simulate tumor dynamics while being treated with DNA damaging chemotherapeutic agent and interacting with other cells and microenvironment. The novel part of the model presented in this thesis is introduction of different drug administration schedules, which enable taking into account the resting intervals for normal cell to recover.
The introduced model was classified by Gevertz et al. as a hybrid, since it combines an agent-based approach to model cancer cell population dynamics and continuous reaction-diffusion partial differential equations to depict oxygen and drug kinetics in the tissue slice. In the model each cell is treated as individual object, which interacts with other cells and microenvironment. This allows to monitor the specific cell properties, among them cell "clonal evolution", at the individual cell level.
Microenvironmental conditions are known to influence tumor development. Cancer cells that are located near the blood vessels are optimally supplied with oxygen, however, they are also exposed to the higher drug concentrations. A small tissue slice, considered in the model, is provided with 4 blood vessels that deliver oxygen as well as drug to the cancer cells. The geometry of the vasculature, which remains unchanged, was designed by by Gevertz et al. as to create the hypoxic regions where tumor cells are deprived from oxygen supply making them switch to the quiescent state. These hypoxic niches and one normoxic region additionally create pharmacological sanctuaries, where drug can not diffuse properly, and are illustrated in Figure 3.1(a). To simplify the modeling, "stromal cells or other extracellular components" were not included in the microenvironment.
Figure 3.1 (c),(d) illustrates model components. Tumor cells are represented by the 65 distinct phenotypes. All simulations observed in the thesis are using the same initial configuration of these 65 cell clones Figure 3.1(b). Further, let $\mathbf{x} = (x, y)$ determine the location of continuous variables, whereas (X, Y) define positions of discrete objects.

3.1 Oxygen kinetics equation

To describe the change in oxygen concentration ξ at point $\mathbf{x} = (x, y)$ in the tumor tissue Gevertz et al. used the reaction-diffusion equation. Oxygen is being supplied from the vasculature V_j (i indexes over the number of vessels with positions $V_j^{(X,Y)}$) at a constant supply rate $S_\xi = 1$. It diffuses with diffusion coefficient D_ξ and is taken up by

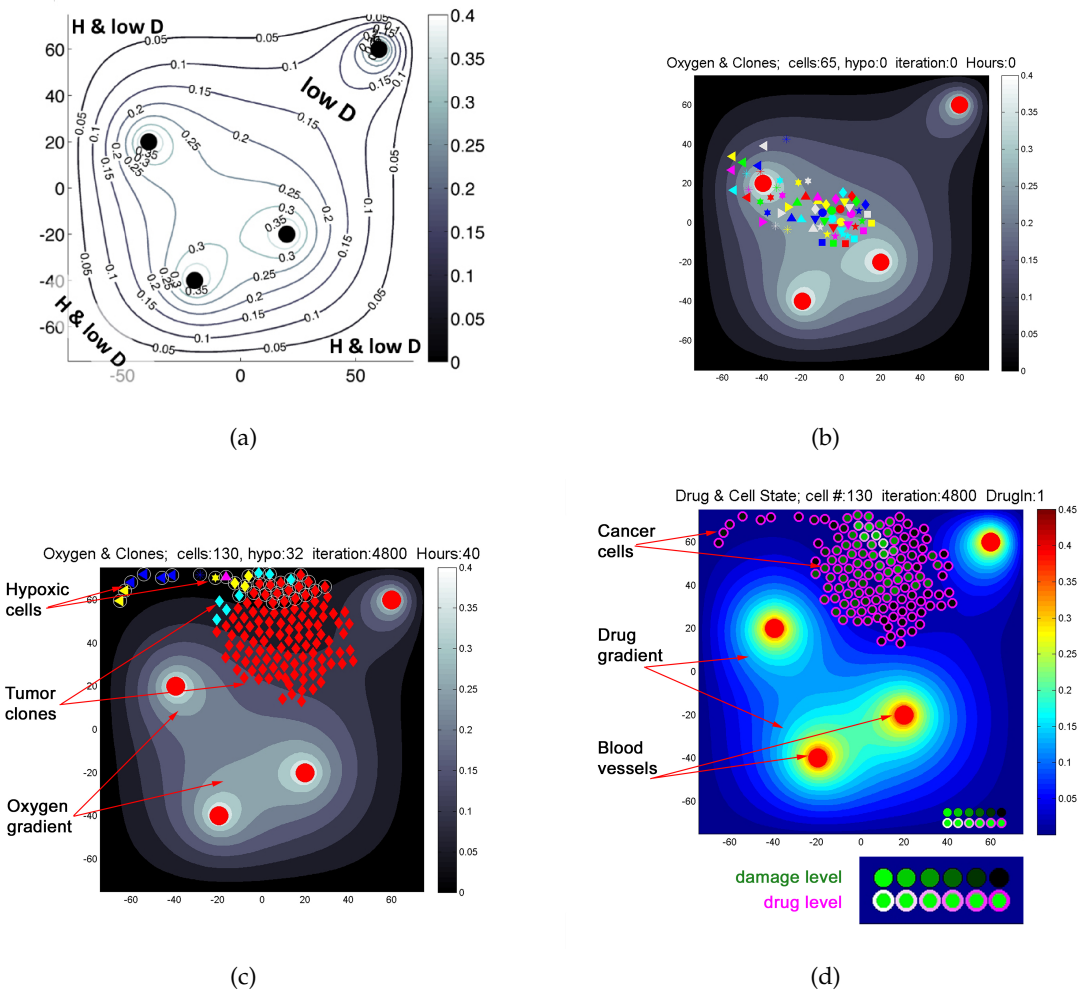

(a) (b)

(c) (d)

Figure 3.1: *Visualization of the model components* In (a) the landscape of the tissue slice is shown, two microenvironmental niches are: a low drug/low oxygen(H&low D)and low drug/normal oxygen (low D). (b) shows the initial configuration of 65 tumor clones. (c) illustrates hypoxic cells, marked with white circles; oxygen gradient as shades of grey and tumor clones, designed with unique phenotypes. (d) shows drug gradient; vasculature and cancer cells, colored with shades of green to present how far from dying the cell is, where contours, drawn with shades of pink, determine drug uptake of the cell.

neighboring tumor cells C_k (k indexes over the number of tumor cells with positions $C_k^{(X,Y)}$) at the uptake rate ρ_ξ. Thus, the equation reads as follows:

$$\frac{\partial \xi(\mathbf{x},t)}{\partial t} = \underbrace{\mathcal{D}_\xi \Delta \xi(\mathbf{x},t)}_{\text{diffusion}} - \underbrace{\min\left(\xi(\mathbf{x},t), \rho_\xi \sum_k \chi C_k(\mathbf{x},t)\right)}_{\text{uptake by the cells}} + \underbrace{S_\xi \sum_j \chi V_j(\mathbf{x},t)}_{\text{supply}} \tag{3.1}$$

The characteristic function χ that determines cells and vessels neighborhood is defined by the fixed cell radius R_C and fixed vessel radius R_V in this fashion:

$$\chi C_k(\mathbf{x},t) = \begin{cases} 1 & \text{if } \left\|\mathbf{x} - C_k^{(X,Y)}(t)\right\| < R_C \\ 0 & \text{otherwise} \end{cases}$$

$$\chi V_j(\mathbf{x},t) = \begin{cases} 1 & \text{if } \left\|\mathbf{x} - V_j^{(X,Y)}(t)\right\| < R_V \\ 0 & \text{otherwise} \end{cases}$$

The sink boundary conditions: $(\partial \xi(\mathbf{x},t)/\partial \mathbf{n} = -\varpi \xi(\mathbf{x},t))$, with $\mathbf{n}$ being the inward pointing normal, are defined for all boundaries of the domain $\mathbf{x} \in \partial\Omega$.
When defining the initial condition, Gevertz et al. set as a goal to imitate the oxygen concentration gradient in the healthy tissue Figure 3.2(a); the other stable gradient was reached for the case of cancer that is not treated with drug (b).

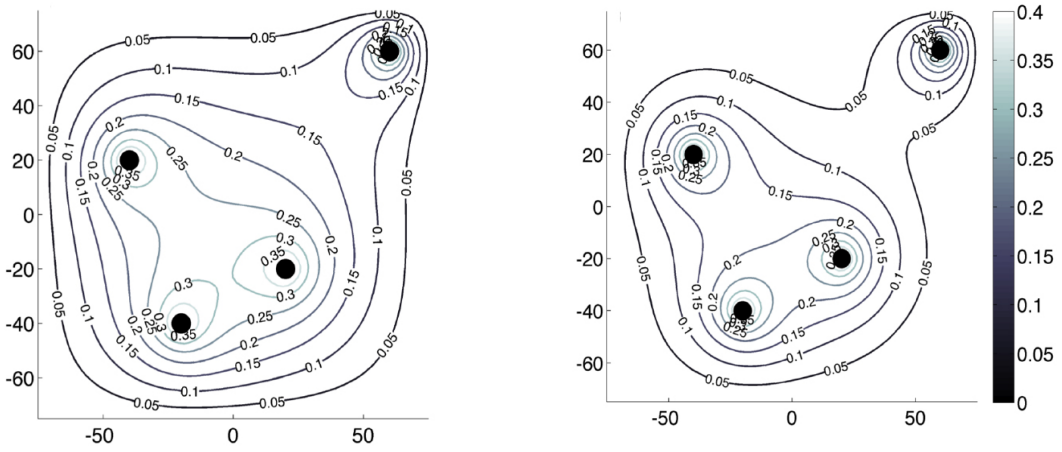

(a) (b)

Figure 3.2: *Stable oxygen* Here (a) and (b) show the initial oxygen distribution in the healthy tissue and while being taken up by the not treated cancer cells respectively.[9]

3.2 Drug kinetics equation

Also change in the drug concentration γ in tumor tissue at point $\mathbf{x} = (x, y)$ was described in [9] by the reaction-diffusion equation. Drug is supplied from the vasculature V_j, diffuses with the diffusion coefficient D_γ, decays at a rate d_γ and at the rate ρ_γ is taken up by neighboring tumor cells C_k. Hence, the equations has the following form:

$$\frac{\partial \gamma(\mathbf{x},t)}{\partial t} = \underbrace{\mathcal{D}_\gamma \Delta\gamma(\mathbf{x},t)}_{\text{diffusion}} - \underbrace{d_\gamma \gamma(\mathbf{x},t)}_{\text{decay}} - \underbrace{\min\left(\gamma(\mathbf{x},t), \rho_\gamma \sum_k \chi C_k(\mathbf{x},t)\right)}_{\text{uptake by the cells}} + \underbrace{S_\gamma \sum_j \chi V_j(\mathbf{x},t)}_{\text{supply}} \tag{3.2}$$

In order to simulate different drug administration protocols, in this thesis the drug supply function S_γ from each vessel was assumed to be a time-dependent piecewise function:

$$S_\gamma = \begin{cases} \gamma & \text{if } t < \frac{T}{n} \\ 0 & \text{if } \frac{T}{n} < t < \frac{2T}{n} \\ \dots \quad \dots & \\ \frac{(-1)^n - 1}{-2}\gamma & \text{if } t > \frac{(n-1)T}{n} \end{cases}$$

where $t \in [0, T]$. To imitate the real-life drug administration regimens, the total treatment time T was divided into the same length fractions and the drug administration intervals were alternated with resting states.
The characteristic function χ and the drug boundary conditions are defined same as for the oxygen concentrations. The initial conditions for the drug concentration were set up this way:

$$\gamma(\mathbf{x}, t_0) = 0 \text{ for } \mathbf{x} \in \Omega \setminus \bigcup V_j \qquad \text{and} \qquad \gamma(\mathbf{x}, t_0) = S_\gamma \text{ for all } V_j^{(X,Y)}.$$

The model was calibrated in [9] as to achieve tumor eradication for the no-resistance case, hence the values for diffusion coefficient D_γ, uptake rate by cancer cells ρ_γ and death threshold Thr_{death} were chosen as to secure this goal.

3.3 Tumor cells dynamics

Owing to the choice of agent-based technique, Gevertz et al. made this model capable to observe each cell separately with the set of its properties that describe cell individual characteristics or represent its interaction with microenvironment. Thus the state of the k-th cell at time t is presented in this fashion:

$$C_k(t) = \left\{ C_k^{(X,Y)}(t), C_k^{age}(t), C_k^{mat}, C_k^{\xi}(t), C_k^{\gamma}(t), C_k^{exp}(t), C_k^{dam}(t), C_k^{death}(t), C_k^{(ID_c, ID_m)} \right\} \tag{3.3}$$

, where $C^{(X,Y)}$ stands for spatial location, C^{age} describes current cell age, C^{mat} cell maturation age, C^{ξ} level of received oxygen, C^{γ} level of accumulated drug, C^{exp} denote the time that cell is being exposed to high drug concentration, C^{dam} is a level of accumulated DNA damage, C^{death} cell death threshold, upon crossing which, cell will die, $C^{(ID_c,ID_m)}$ shows unique indices of the current cell ID_c and its mother cell, to enable the cell history tracking.
The spatial location $C^{(X,Y)}$ of each initial cell is predefined. The positions of daughter cells will be determined upon division and cell-to-cell interaction. The age of each cell gets incremented by Δt after each time step: $C_k^{age}(t+\Delta t) = C_k^{age}(t) + \Delta t$ The ability of cell to divide depends on its maturity and microenvironmental conditions. Cell proliferation process can start after cell has reached maturation age and there is enough space in the neighborhood to divide, otherwise it will be suppressed until these conditions are met. Division is modeled by splitting the C_k cell and creating C_{k1} and C_{k2}, where one cell will inherit the position of the mother cell and the other one will be placed randomly nearby, using aa random angle θ:

$$C_{k1}^{(X,Y)}(t) = C_k^{(X,Y)}(t) \qquad \text{and} \qquad C_{k2}^{(X,Y)}(t) = C_k^{(X,Y)}(t) + R_C(\cos(\theta), \sin(\theta)) \tag{3.4}$$

The age of the newly created cells is set to zero $C_{k1}^{age}(t) = C_{k2}^{age}(t) = 0$, whereas the maturation age will be accepted from the mother cell with a gentle noise term: $C_{k1}^{mat}(t)$, $C_{k2}^{mat}(t) = C_k^{mat} \pm \omega$, where $\omega \in [0, C_k^{mat}/20]$. Inherited from the mother cell will be also the DNA damage level $C_{k1}^{dam}(t) = C_{k2}^{dam}(t) = C_k^{dam}(t)$, as well as the cell death threshold $C_{k1}^{death}(t) = C_{k2}^{death}(t) = C_k^{death}(t)$ along with the drug exposure time $C_{k1}^{exp}(t) = C_{k2}^{exp}(t) = C_k^{exp}(t)$. While, the level of accumulated drug will be divided evenly between the daughter cells $C_{k1}^{\gamma}(t) = C_{k2}^{\gamma}(t) = 0.5 \times C_k^{\gamma}(t)$. Regarding the level of sensed oxygen, $C_{k1}^{\xi}(t)$ and $C_{k2}^{\xi}(t)$ will be separately determined based on the oxygen level in the cell neighborhood. The unique cell index, identifying cell heritage, consists of the new index for current cell and the mother cell index $C_{k1}^{(ID_c,ID_m)} = (k_1, C_k^{ID_c})$ and $C_{k2}^{(ID_c,ID_m)} = (k_2, C_k^{ID_c})$. The inheritance routine is illustrated in Figure 3.3. The update of the cell state, which happens in random cell order, is conditioned by its response to the microenvironment. Based on the cell location in relation to blood vessels geometry, it receives a particular amount of drug and oxygen. Depending on the oxygen level cell may potentially proliferate or will switch to the quiescent state, whereas drug level determines if cell will survive, acquire resistance or die. Some of the cell properties will be inherited from mother cell upon cell division. Cell responses to microenvironmetal conditions are summarized and illustrated in Figure 3.3.
From the vasculature each cell is supplied with oxygen (ξ) and drug (γ). The k-th cell inspects its local neighborhood, defined as $\left\{\mathbf{x} : \left\|\mathbf{x} - C_k^{(X,Y)}\right\| < R_C\right\}$, and consumes C_k^{ξ} and C_k^{γ} of sensed oxygen and drug respectively:

$$C_k^{\xi}(t+\Delta t) = \underbrace{\sum_{\mathbf{x}} \xi(\mathbf{x}, t)}_{\text{sensed and used}} \tag{3.5}$$

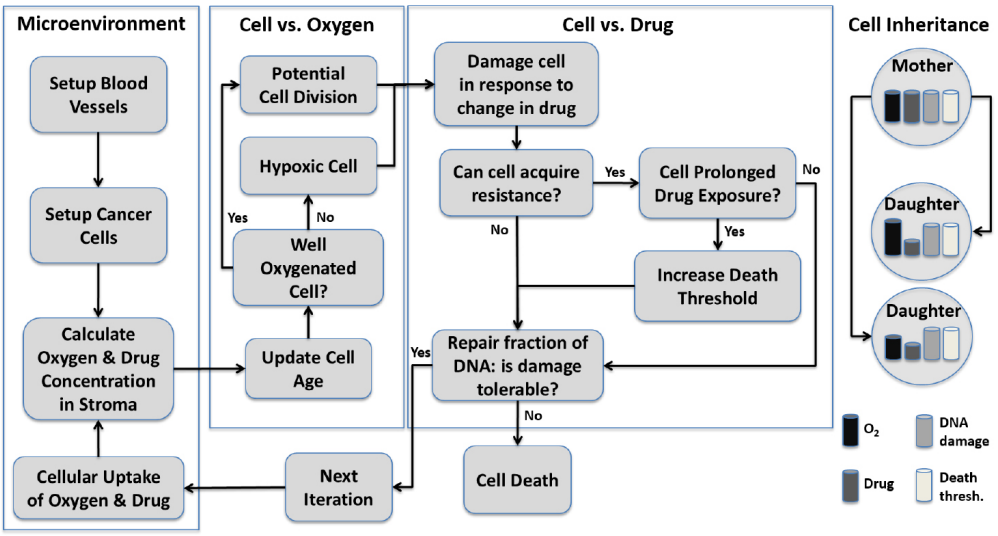

Figure 3.3: *Cell interaction with microenvironment* [9]

$$C_k^{\gamma}(t+\Delta t) = C_k^{\gamma}(t) + \left[\max\left(0, \sum_{\mathbf{x}} \underbrace{\min(\gamma(\mathbf{x},t),\rho_{\gamma})}_{\text{uptake}} - \underbrace{d_{\gamma} C_k^{\gamma}(t)}_{\text{decay}} \right) \right], \tag{3.6}$$

where C^{ξ} determines cell proliferative capabilities, with cell switching to resting state if level of sensed oxygen is below hypoxia threshold Thr_{hypo}. Being exposed to drug cell suffers DNA damage, the degree of which depends on the duration of drug exposure and the drug concentration. However, cancer cells are self-renew and therefore have an active DNA-repair capacity. Moreover, they can become resistant being subjected to cytotoxic drug over time. These observations were presented in [7] and adopted in the model, used in this thesis. Thus, cell damage level is calculated as follows:

$$C_k^{dam}(t+\Delta t) = C_k^{dam}(t) + \left[\max\left(0, \sum_{\mathbf{x}} \underbrace{\min(\gamma(\mathbf{x},t),\rho_{\gamma})}_{\text{uptake}} - \underbrace{d_{\gamma} C_k^{\gamma}(t)}_{\text{decay}} \right) \right] \Delta t - \underbrace{p C_k^{dam}(t)}_{\textbf{repair}} \tag{3.7}$$

A cell will die if its damage exceeds the death threshold that in its turn depends on the resistance type (no-resistance, acquired resistance). In no-resistance case, cell death threshold is a constant $C_k^{death} = Thr_{death} = 0.5$. Whereas, the process of acquiring resistance was modeled as an individual ability of each cell to increase its death threshold independently by $increment\_size$ parameter value under prolonged drug exposure.

$$C_k^{death}(t+\Delta t) = \begin{cases} C_k^{death}(t) + \Delta_{death} & \text{if } C_k^{exp}(t) > t_{exp} \\ C_k^{death}(t) & \text{otherwise} \end{cases}$$

Hence, death threshold will be incremented if C^{exp} is above the critical amount of time t_{exp}, where C^{exp} gets increased if amount of drug taken up in previous time point exceeds the drug concentration threshold γ_{exp}.

$$C_k^{exp}(t+\Delta t) = \begin{cases} C_k^{exp}(t) + \Delta t & \text{if } C_k^{\gamma}(t) > \gamma_{exp} \\ 0 & \text{otherwise} \end{cases}$$

Initial conditions of the system are set as follows:

$$C_k(t_0) = \left\{ (X_k, Y_k), 0, M_k, \sum_{\mathbf{x}} \xi(\mathbf{x}, t_0), 0, 0, 0, T_k, (k, 0) \right\} \tag{3.8}$$

All cells have predefined spatial locations (X_k, Y_k), as it is shown in Figure 3.1(b). Initial age is set to zero, while maturation age is set to M_k, where M_k drawn from a uniform distribution $[0.5 \times Age, 1.5 \times Age]$ with Age being the average maturation age. As it was mentioned before, the model was calibrated as to have a numerically stable oxygen gradient in healthy tissue. Thus the initial level of sensed oxygen will be defined according to its concentration in the cell neighborhood. Since there is no drug in the domain, initially the level of sensed drug, as well as the drug exposure time and the cell damage level are set to zero. The death threshold for both no-resistance and acquired resistance case is set to $T_k = Thr_{death}$. All the initial cells have unknown mothers, hence the unique cell index is defined in this fashion: $(k, 0)$, where the first entry will be inherited by the cell's daughters as their mother cell index.

3.4 Equations of cell mechanics

As it was mentioned before, changes in cell position are determined by cell division and the interaction with other cells. Thus in this subsection the equations, which model cell mechanics are presented. The model has adopted a particle-spring system, which determine cancer cells as particles with assigned elastic springs generating forces whenever displaced from the equilibrium. Using the approach by [24, Meineke et al. 2001], each cell within the tissue slice is represented by the coordinates of the center of its nucleus and its radius R_C. Therefore, each cell is assumed to occupy a predefined volume in the domain and preserve it throughout its lifetime. Two cells are said to come into contact with each other if the distance between them is lesser than the cell diameter $2R_C$. Whenever two cells $C_i^{(X,Y)}(t)$ and $C_j^{(X,Y)}(t)$ interact, two repulsive forces (linear, Hookean) $f_{i,j}$ and $-f_{i,j}$ will be applied to these cells respectively, pushing them away from each other while maintaining cells' volumes:

$$f_{i,j} = \begin{cases} \mathcal{F}(2R_C - \|\mathbf{X}_i - \mathbf{X}_j\|)\frac{\mathbf{X}_i - \mathbf{X}_j}{\|\mathbf{X}_i - \mathbf{X}_j\|} & \text{if } \|\mathbf{X}_i - \mathbf{X}_j\| < 2R_C \\ 0 & \text{otherwise} \end{cases}$$

,

where $\mathbf{X}_i = C_i^{(X,Y)}(t)$ for simplicity, with F being the constant spring stiffness and $2R_C$ being the spring resting length. In case the cell $\mathbf{X}_i$ has more then one cell $\mathbf{X}_{j1}, \ldots, \mathbf{X}_{jM}$ in its neighborhood, then the total force F_i acting on $\mathbf{X}_j$ is equal to the sum of all forces $f_{i,j1}, \ldots, f_{i,jM}$ coming from the string of all neighboring cells that are connected to the cell $\mathbf{X}_i$:

$$F_i = \underbrace{\mathcal{F}(2R_C - \|\mathbf{X}_i - \mathbf{X}_{j1}\|)\frac{\mathbf{X}_i - \mathbf{X}_{j1}}{\|\mathbf{X}_i - \mathbf{X}_{j1}\|}}_{f_{i,j_1}} + \cdots + \underbrace{\mathcal{F}(2R_C - \|\mathbf{X}_i - \mathbf{X}_{jM}\|)\frac{\mathbf{X}_i - \mathbf{X}_{jM}}{\|\mathbf{X}_i - \mathbf{X}_{jM}\|}}_{f_{i,j_M}} \tag{3.9}$$

Therefore the movement of a cell is determined by the local repelling and attracting forces that can be modeled by a network of springs connecting adjacent cells, which are assumed to be overdamped, hence the system will return to the equilibrium without oscillations. The cell dynamics is controlled by the Newtonian equations, thus the force and the effective displacement within a small time interval Δt are given by:

$$F_i = -\nu\frac{d\mathbf{X}_i}{dt} \qquad \text{and} \qquad \mathbf{X}_i(t + \Delta t) = \mathbf{X}_i(t) - \frac{1}{\nu}\Delta t F_i \tag{3.10}$$

where $\mathbf{X}_i$ is the center of the i-th cell and ν is the damping constant.
Upon division two daughter cells are created. As the distance between them is lesser than $2R_C$ the repulsive forces are activated. This may end up daughter cell being placed near other cells, thus again activating the repulsive forces. Consequently, until all cells are pushed away and the whole tumor population reaches an equilibrium configuration, multiple repulsive forces might be applied. Some of the cells will be thrown out of the domain, when the population reaches its equilibrium. These cells are not considered in the analysis. Modeling of cell-to-cell interaction allows tracking the amount of adjacent cells. Thus, the overcrowding condition can be determined, which will decide the further population growth, as a cell divides only if there is enough space in the neighborhood. Model parameters defining cell mechanics are presented in Table 3.1.

Cellular parameters	
Cell radius	$R_C = 5\mu\text{m}$
Spring stiffness	$F = 1mg/s^2$
Mass viscosity	$\nu = 15mg/s$
Overcrowding	$Neighbors = 14\text{cells}$
Maturation age	$Age = 360\text{min} \pm \text{noise} \in [0, Age/20]$

Table 3.1: Parameters of cell mechanics

3.5 Parameter space

Since the main goal of the anticancer therapy is to eliminate tumor, the conditions under which cancer cell apoptosis is induced are of particular interest. Thus, in this subsec-

tion the parameter regimes for which the level of accumulated damage C^{dam} by a cell surpasses its death threshold C^{death} are investigated.
It was assumed that all the cells incurs identical amount of DNA damage. Thus, at any fixed time point t, all cell carry the same amount of DNA damage $x(t) = C_k^{dam}(t)$. Let $\eta(t) > 0$ be the new amount of the incurred damage in each cell at time t and $0 \leq p \leq 1$ is defined as the constant fraction of DNA damage that will be repaired. Hence, at any time point $t > 0$ for a small h the spatially-constant damage level can be represented as:

$$x(t) = x(t-h) + \int_{t-h}^{t} \eta(s)\mathrm{d}s - \int_{t-h}^{t} px(s)\mathrm{d}s \tag{3.11}$$

Applying the Fundamental Theorem of Calculus one can reduce this equation to:

$$\dot{x}(t) = \eta(t) - px(t) \tag{3.12}$$

Assuming that there is no damage $x(0) = 0$ at the beginning $t = 0$ of the treatment, the solution of the Equation 3.12:

$$x = \mathrm{e}^{-pt}K(t)$$

$$\dot{K}(t) = \mathrm{e}^{pt}\eta(t) \Rightarrow K(t) = \int_0^t \mathrm{e}^{ps}\eta(s)\mathrm{d}s$$

$$x(t) = \left(\int_0^t \mathrm{e}^{ps}\eta(s)\mathrm{d}s\right)\mathrm{e}^{-pt} \tag{3.13}$$

The amount of the new incurred damage in each cell is determined by the cell location and the amount of drug it can sense and uptake, and the drug exposure time. Yet, as the drug influx from the vessels is constant on each interval the amount of damage will be bounded from above and thus assumed to be constant $\eta(t) = \eta$. For $p \neq 0$ Equation 3.13 transforms:

$$x(t) = \frac{\eta}{p}(1 - \mathrm{e}^{-pt}) \tag{3.14}$$

When there is no damage repair $p = 0$ Equation 3.13 becomes:

$$x(t) = \eta t \tag{3.15}$$

Numerical simulations revealed that the microenvironmental niches have a great impact on the tumor development and thus treatment outcome. Consider the acquired resistance case $\alpha = \Delta_{death} \neq 0$ with fixed constant death threshold $\beta = Thr_{death}$, the new amount of incurred damage $\eta > 0$ and p fraction of damage repaired. Then the death threshold will be incremented as follows $C^{death}(t) = \alpha t + \beta$.In [9] was formulated and proved a proposition that determines a condition for which, ignoring the spatial component, tumor eradication $x(t) = C_k^{dam}(t) > C^{death}(t)$ can be achieved.

Proposition 3.5.1. *If $\alpha < \eta$ and $0 < p < \frac{\eta}{\beta}$, then $\exists\, \alpha* < \alpha$, $T_1(\alpha*)$ and $T_2(\alpha*)$ such that $\forall$ $T_1(\alpha*) < t < T_2(\alpha*)$ the damage level satisfies $x(t) > \alpha t + \beta$ and thus, all cells die.*

Proof. Let $F(t) := x(t) - \alpha t - \beta$. Substituting this into the Equation 3.14 gives:

$$F(t) := \frac{\eta}{p} - \alpha t - \beta - \frac{\eta}{p}\mathrm{e}^{-pt}.$$

Note that $F(0) = -\beta < 0$ and $F'(t) = \eta \mathrm{e}^{-pt} - \alpha$. $F'(t) = 0$, then $\mathrm{e}^{-pt} = \frac{\alpha}{\eta} \Rightarrow t* = -\frac{1}{p}\ln\frac{\alpha}{\eta}$. Since $\alpha < \eta$:

$$F'(t) = \begin{cases} \geq 0 & t \leq t* \\ 0 & t = t* \\ \leq 0 & t \geq t* \end{cases}$$

Thus the behavior of $F(t)$ depends on the size of parameter α Figure 3.4. If for some

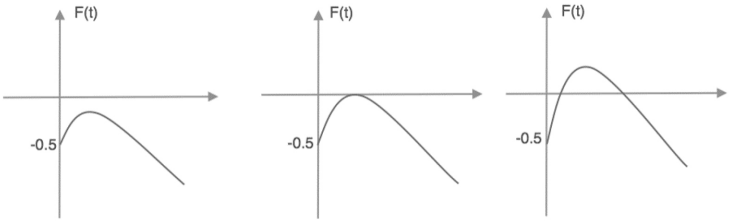

Figure 3.4: *Dependence of the F function behavior on the parameter* α [9]

$\alpha < \eta$, $F(t*) > 0$, then there exists an interval (T_1, T_2), such that for $t \in (T_1, T_2)$, $F(t) > 0$, i.e., $x(t) > \alpha t + \beta$. Consequently, one should look for such $\alpha < \eta$ that $F(t*) > 0$. Let $F(t*) = G(\alpha) =: \frac{\eta}{p} - \beta\frac{\alpha}{p}\left(1 - \ln\frac{\alpha}{\eta}\right)$, then

- $\lim_{\alpha\to 0^+} G(\alpha) = \frac{\eta}{p} - \beta = \begin{cases} > 0 & p < \frac{\eta}{\beta} \\ < 0 & p > \frac{\eta}{\beta} \end{cases}$
- $\lim_{\alpha\to\eta^-} G(\alpha) = -\beta < 0$
- on $(0, \eta)$, $G'(\alpha) = \frac{1}{p}\ln\frac{\alpha}{\eta} < 0$

Hence, if $p < \frac{\eta}{\beta}$, by Intermediate Value Theorem, there exists $0 < \alpha* < \eta$ such that $G(\alpha*) = 0$, and $G(\alpha) > 0$ for $\alpha < \alpha*$, and $G(\alpha) < 0$ for $\alpha > \alpha*$. Thus, if $p < \frac{\eta}{\beta}$, and $\alpha < \alpha*$, then $F(t*) > 0$, and there exist T_1, T_2 that depend on $\alpha*$, such that for $T_1 < t < T_2$, $F(t) = x(t) - \alpha t - \beta > 0$. □

Therefore from Proposition 3.5.1 it follows that if $p < \frac{\eta}{0.5} < 6 \times 10^{-4}$ and if $\alpha < \eta < 3 \times 10^{-4}$ (both upper bounds fixed using the model parameters) then all tumor cells will be killed by the drug. For the numerical simulation a value for DNA repair rate p was chosen from this range $p = 1.5 \times 10^{-4}$. As for the $increment\_sizes$ parameter, in simulations three different values were considered for the acquired resistance case: $3.5 \times 10^{-5}, 4.5 \times 10^{-5}, 5.9 \times 10^{-5}$. All of them lie in range suggested by the Proposition 3.5.1, however, the simulations for acquired resistance case presented in this thesis not

always show the complete tumor eradication. This can explained by the assumption made for the level of incurred damage η in each time point to be a constant for all cells, despite of η being a function depending on time and space. Substituting the repair rate value used in the simulations $p = 1.5 \times 10^{-4}$ and considering the condition for tumor eradication $p < \frac{\eta}{0.5}$ one will get the value range for the incurred damage $\eta > 7.5 \times 10^{-5}$ that ensures the successful treatment outcome.
Yet it would be mistake to overlook the fact that cells positioned far away from the blood vessels will absorb lower amount of drug, and hence will get less damage. Thus these cells can not fulfill $\eta > 7.5 \times 10^{-5}$ condition, as incurred damage for them will be smaller. Consequently the numerical simulations for them will not provide the theoretically anticipated result. Hence, it is obvious that spatial component has a great impact on the tumor development and should not be ignored.
To analyze the impact of microenvironmental niche on the treatment outcome, the investigation of the acquired resistance case is provided in [9]. It has revealed that microenvironment greatly affects disease development for small $increment\_sizes$ selecting cells from low-drug normoxic niche to be the persistent clones that will stay longer in the domain and in some cases eventually survive the treatment course. Whereas for the large values its role is reduced as cancer cells acquire resistance to the medication very fast resulting in heterogeneous tumor composed of different clones coming from all over the tissue slice. The further investigation of this issue is provided in chapter 4.

3.6 Numerical implementation

The implemented in MATLAB software by Gevertz et al. aforementioned model was extended with updated drug supply function for this thesis purposes. The domain is discretized into a square grid with mesh width h_b. The time is also discrete with a time step Δt. Table 3.2 shows the numerical values of the mentioned parameters.
The solutions of the reaction-diffusion partial differential equations describing the oxy-

Domain size	$[-75, 75] \times [-75, 75] \mu\text{m}$
Mesh width	$h_b = 2\mu\text{m}$
Time step	$\Delta t = 0.5\text{min}$

Table 3.2: Numerical parameters [9]

gen and drug kinetics are approximated by means of the finite difference method, with forward-difference approximation (in time) on a square grid (centered in space) using sink-like boundary conditions. The initial oxygen and drug concentrations $\xi(\mathbf{x}, t_0)$ and $\gamma(\mathbf{x}, t_0)$ respectively are presented in Table 3.3. Further, at each time step concentrations $\xi(\mathbf{x}, t + \Delta t)$ and $\gamma(\mathbf{x}, t + \Delta t)$ will be approximated using the values from the previous step are used $\xi(\mathbf{x}, t)$ and $\gamma(\mathbf{x}, t)$. The interaction of a cell with oxygen and drug concentrations is modeled at the same discretized time points for which the solutions of partial differential equations are approximated. Thus, at each time point, every discrete grid

Metabolite kinetics (normalized values)		
	Oxygen	Drug
Supply rate	$S_\xi = 1$	S_γ varies
Diffusion coefficient	$D_\xi = 0.5$	$D_\gamma = 0.5$
Decay rate	none	$d_\gamma = 1 \times 10^{-4}$
Boundary outflux rate	$\varpi = 0.45$	$\varpi = 0.45$
Cellular uptake	$\rho_\xi = 5S_\xi \times 10^{-5}$	$\rho_\gamma = S_\gamma \times 10^{-4}$
Threshold value	$Thr_{hypo} = 0.05$	$Thr_{hypo} = 0.5$

Table 3.3: Non-dimensionalized parameters of oxygen and drug kinetics based on model calibration [9]

point, which is located within a cell radius distance from the tumor cell center can uptake drug or oxygen from the environment at an uptake rate ρ_γ or ρ_ξ respectively. In case the amount of drug (oxygen) in the cell's neighborhood is not enough to take up ρ_γ (ρ_ξ) units, then all available drug (oxygen) will be taken up by the cell. The absorbed oxygen will be right away used by the cell, whereas the drug taken up by the cell will decay at the same decay rate it does in the microenvironment. The cell-drug interaction parameters are presented in Table 3.4. In case of no-resitance as well as in case of

Death thresh. incr.	No-resistance $\Delta_{death1} = 0$	Acquired resistance $\Delta_{death2} = 3.5 \times 10^{-5}$ $\Delta_{death3} = 4.5 \times 10^{-5}$ $\Delta_{death4} = 5.9 \times 10^{-5}$
Death thresh. mult.	$Thr_{multi} = 1$	
Drug exposure level	$\gamma_{exp} = 0.01$	
Drug exposure time	$t_{exp} = 5\Delta t$	
DNA repair	$p = 1.5 \times 10^{-4}$	

Table 3.4: Cell-drug interaction parameters

acquired resistance cancer cells have the same tolerance to the drug damage Thr_{multi}. Cancer cells will also steadily repair their DNA damage at a repair rate p. As the Δ_{death} parameter value is set to 0 for the no-resistance tumor its death threshold will not increase throughout the treatment course, whereas in acquired resistance case it will be continuously incremented if prolonged drug exposure conditions are met.

4 Analysis of Results

This chapter presents the analysis of the data obtained through simulations of different DNA damaging drug administration schedules. Since the dynamics of cancer cells caused by the drug regimens is the focus of interest, a set of conditions should be defined: all simulations have the same initial configuration of the 65 tumor cells and 4 vessels Figure 3.1, no pre-existing resistance present and, to ease the interpretation of results, emergence of resistance due to a drug exposure only (no random mutations occur) was considered.The presented analysis investigates the numerical simulations of tumor behavior under different drug administration protocols for no-resistance and acquired resistance cases, gives insight into cancer phylogenetic trees and determines reasonable drug dose by the means of drug response curves.

4.1 Drug Administration Regimens

Here, the tumor dynamics while being subjected to the DNA damaging drug treatment is considered. As stated in chapter 3 a time-dependent drug supply function is assumed to be a piecewise constant function reflecting the real-life chemotherapy routine with drug administration and resting intervals in the cycle of treatment.
It is known, that chemotherapeutic drugs are toxic to cancer cells, but they also dangerous for normal cells. Thus toxicity issue is of the most concern, while designing treatment protocols. To ensure that patient will be able to tolerate side effects of medications, constrains on drug dose (maximum tolerable dose) and cumulative drug toxicity are usually used. A possible approach to bind drug dose is to examine the overall amount of drug introduced to the system.
Consider the case of continuous drug supply with the fixed number of iterations (Niter). Medications are being steadily administrated from the 4 vessels, thus [$Niter \times 4 \times DrugIn$] units of drug would be introduced. Drug supply concentration of $DrugIn = 1$ used in the model, is a normalized value based on the model calibration. Further this overall drug amount introduced to the tumor being continously delivered would be compared with the ones obtained through applying different drug regimens.
While planning chemotherapy regimen in the real-life resting intervals and drug administration are often adjusted to the cell cycle as to get the highest possible damage to the cancer cells and give normal cells an opportunity to recuperate. Therefore, in order to obtain a simulation of a more realistic cancer treatment scenario, it was decided to include the time for normal cell to recover. The resting intervals were introduced to the system by dividing the whole treatment time into same length fractions alternating

drug delivery with no drug intervals. Cases with 2, 3 and 4 fractions were investigated. The decision on the drug dose delivered per interval was made in such a way so as not to exceed the overall amount of drug introduced in the continuous case. The concentrations, same for all intervals, were defined as follows: for even number of intervals:

$$\frac{Niter}{2n} \times 4 \times DrugIn + \frac{Niter}{2n} \times 4 \times 0 + \cdots + \frac{Niter}{2n} \times 4 \times 0 \leq Niter \times 4 \times 1$$
$$\Rightarrow \frac{nNiter}{2n} \times 4 \times DrugIn \leq Niter \times 4 \times 1 \Rightarrow DrugIn \leq 2$$

for odd number of intervals:

$$\frac{Niter}{2n+1} \times 4 \times DrugIn + \frac{Niter}{2n+1} \times 4 \times 0 + \cdots + \frac{Niter}{2n+1} \times 4 \times DrugIn \leq Niter \times 4 \times 1$$
$$\Rightarrow \frac{(n+1)Niter}{2n+1} \times 4 \times DrugIn \leq Niter \times 4 \times 1 \Rightarrow DrugIn \leq 1 + \frac{n}{n+1}$$

for the special case, when drug is administrated only in the first interval:

$$\frac{Niter}{n} \times 4 \times DrugIn + \frac{Niter}{n} \times 4 \times 0 + \cdots + \frac{Niter}{n} \times 4 \times 0 \leq Niter \times 4 \times 1$$
$$\Rightarrow DrugIn \leq n$$

Thus maximal concentrations are set. Struggling to reduce toxicity, lower drug doses were also considered. As mentioned before, little is still known about the best possible DrugIn value to be used in the model, although it might be estimated through the analysis of the numerical simulations. Furthermore in this section, through comparing continuous case with other drug regimens, the investigation on the minimal overall amount of drug needed to eradicate the tumor is presented .

4.1.1 No Tumor Resistance

The observations of the no resistance case are presented here. Since the initial tolerance to drug damage Thr_{multi} (multiply_death=1) cannot increase during treatment, as the $increment\_sizes$ parameter is set to 0, it is ensured that no anti-cancer drug resistance may occur. All simulations differ only in the way the drug is administrated, initial conditions and the parameter values are the same. The original death threshold for cells ($Thr_{death} = 0.5$) is constant here and DNA repair rate is ($p = 1.5 \times 10^{-4}$).
Firstly, consider the case of continuous drug supply with dose intensity DrugIn set to 1. Owing to the model being calibrated accordingly, this case is an example of successful tumor eradication. The behavior of the cancer cell population is shown in the Figure 4.1(a), in the onset of the treatment (i), though cells are accumulating damage Figure 4.1(b), the effect of drug is not enough to eradicate the tumor. Hence, the cell population increases in size (ii), however, at this time the accumulated damage of the most of the cells reaches threshold and the greater part of the population dies, with only small part of it (iii), located in the low drug niche, being able to survive. These remaining cells manage to increase the cell population size (vi). But, even so, one can

see from the snapshots Figure 4.1(c), that the majority of cells through the time interval (iii-vi) is colored with the dark shade of green indicating its high level of damage, thus they die out eventually. The amount of iterations needed to eradicate the tumor, while administrating drug continuously with $DrugIn = 1$, is 6607. Thus the overall amount of drug introduced to the system is $6607 \times 4 \times 1 = 26428$ units of drug.

Next, examine the impact of including the time for normal cells to recover. How-

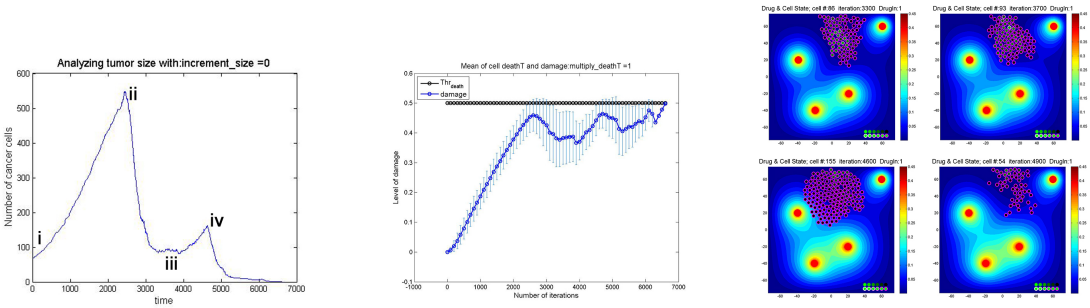

(a) Cancer size (b) Damage curve (c) Cell dynamics for (iii)

Figure 4.1: *Continuous no-resistance case.* Cancer cells population dynamics and damage accumulation curves are shown in (a) and (b) respectively. In (c) the snapshots of phases of cancer size increase and eventual eradication corresponding to (iii) and (iv) are shown. Figure 4.1(b) shows the mean value of accumulated damage of all cells with vertical lines, representing standard deviation, and an average death threshold of all cancer cells (constant in this case).

ever, prior to introducing the resting intervals, the amount of iterations should be fixed. Based on the outcome for the continuous case, it seems reasonable, therefore, to decide on number that is at least satisfies: $\frac{Niter}{2} < 6607$, otherwise one would fail to see the effect on applying different drug protocols. As, in case $Niter > 6607$, the result of division into 2 fractions will duplicate the outcome for the continuous case. Thus, the iteration number was set to 8000. Then the overall drug amount should not exceed $8000 \times 4 \times 1 = 32000$. Like it was mentioned before, in this thesis investigated was the division into 2, 3 and 4 fractions. The results of simulations performed for the no-resistance case are summarized in Table 4.1.

In Table 4.1 successful drug administration regimens with complete tumor eradication are marked with green color. Cases, marked with blue font, are the cases where the overall toxicity level is lesser than the expected one 32000, be it due to the low drug dose or tumor eradication faster than planned. Failed treatment cases have the amount of iterations 8000 and the total amount of drug equals to the planned one $\frac{8000}{n} \times 4 \times DrugIn + \frac{8000}{n} \times 4 \times 0 + \ldots$, therefore omitted in Table 4.1.
Successful treatment schedules, with the exception of the case 1-0, follow the same scenario. Cell evolution curves and damage plots will be quite similar for all these cases Figure 4.2. The cancer cell population being exposed to the drug will at first increase

DrugIn \ Intervals	1 D	2 D-0	3 D-0-0	3 D-0-D	4 D-0-D-0
0.5		587 9		350 13	423 19
1	0 6607 26428 0	0 7563 16000 0		94 1	128 1
1.5		0 3368 20208 0		0 3368 16000 0	0 4281 13686 0
2		0 3214 25712 0			0 3214 16000 0
3			0 3157 32000 0		

Table 4.1: *No-resistance case.* The cases of successful tumor eradication and cases with overall amount of drug lesser than 32000 are marked with green background color and blue font color respectively. Table entries: number of survived cells, number of iterations (omitted in case of failed treatment), overall amount of drug (omitted in case of failed treatment), number of survived clones.

in size, however, owing to the relatively high dose intensity $DrugIn > 1$, it fast accumulate enough damage to reach the death threshold and consequently die out. Thus, comparing cell evolution curve for these cases Figure 4.2(a) with the one for continuous treatment Figure 4.1(a), one can see that even that cell subpopulation, which was able to temporally escape death and regrow thanks to the low drug niche (iii-vi) in continuous case, now due to the higher drug concentration is nowhere to be found.

As for the case 1-0, the cell population behavior replicates the continuous case with all 4 phases of cancer cells population dynamics curve Figure 4.1(a), although this time tumor gets eradicated a bit later, after 7563 iterations. This is already promising result as the overall toxicity was reduced while maintaining the same drug dosage.

Of particular interest are the failed treatment cases, they are 0.5 and 1 dose intensity "families". Firstly, consider the $DrugIn = 1$-family of drug administration regimens Figure 4.3. In both protocols one clone, initially located in the low drug niche survives. Compared to the continuous case Figure 4.1(a) both populations Figure 4.3(a) and Figure 4.3(c) have similar dynamics with regrowing subpopulation (i-iv), but due to the continuous DNA damage repair and zero drug supply in the resting intervals, tumor

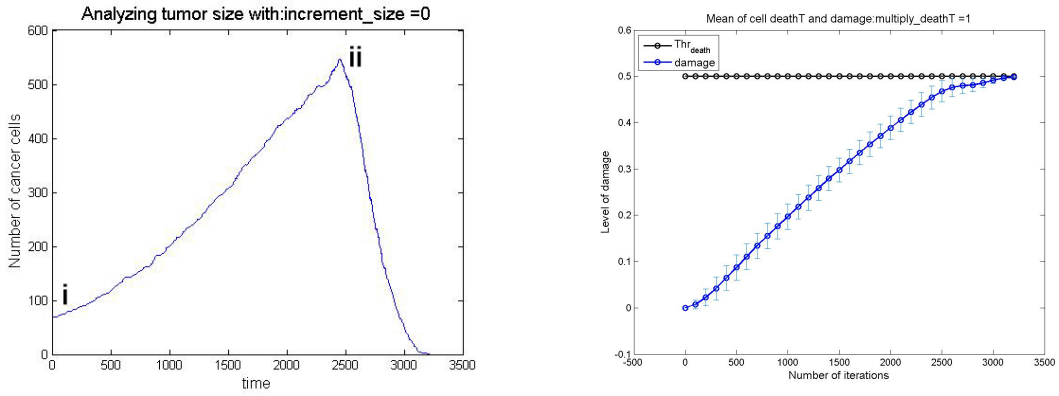

(a) Cancer size (b) Damage curve

Figure 4.2: *Successful treatment* Cancer cells population dynamics and damage accumulation curves are shown in (a) and (b) respectively. Figure 4.2(b) shows the mean value of accumulated damage of all cells with vertical lines, representing standard deviation, and an average death threshold of all cancer cells (constant in this case).

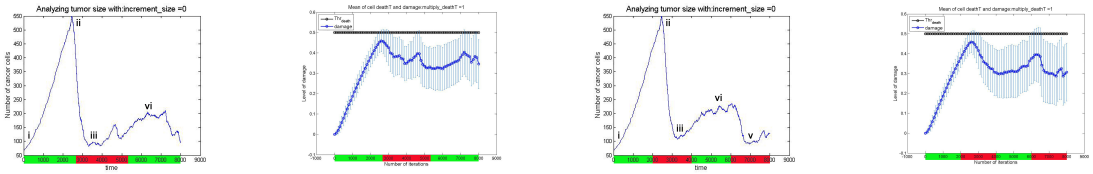

(a) 1-0-1 (b) 1-0-1 (c) 1-0-1-0 (d) 1-0-1-0

Figure 4.3: $DrugIn = 1$ *family, failed treatment.* Cancer cells population dynamics and damage accumulation curves for the drug regimens 1-0-1 and 1-0-1-0 are shown in (a,c) and (b,d)respectively. Figure 4.3(b) and Figure 4.3(d) show the mean value of accumulated damage of all cells with vertical lines, representing standard deviation, and an average death threshold of all cancer cells (constant in this case). Drug administration and resting intervals are colored green and red respectively.

doesn't accumulate enough damage to be eradicated at the iteration 8000. In case of 1-0-1-0 regimen, repopulation of cancer cells (iv) and then decrease in size is again followed by the escape in the low drug niche (v) and potential regrow further.
As for the $DrugIn = 0.5$-family, poor treatment results can be explained by the too low dose intensity. In either of cases cancer cells fail to accumulate enough damage to exceed the death threshold as shown in Figure 4.4. Cancer population size curves show different behavior based on the protocol. One can notice, that each resting interval is accompanied by the tumor regrow.

Analysis revealed that $DrugIn > 1$ protocols show better results compared to those

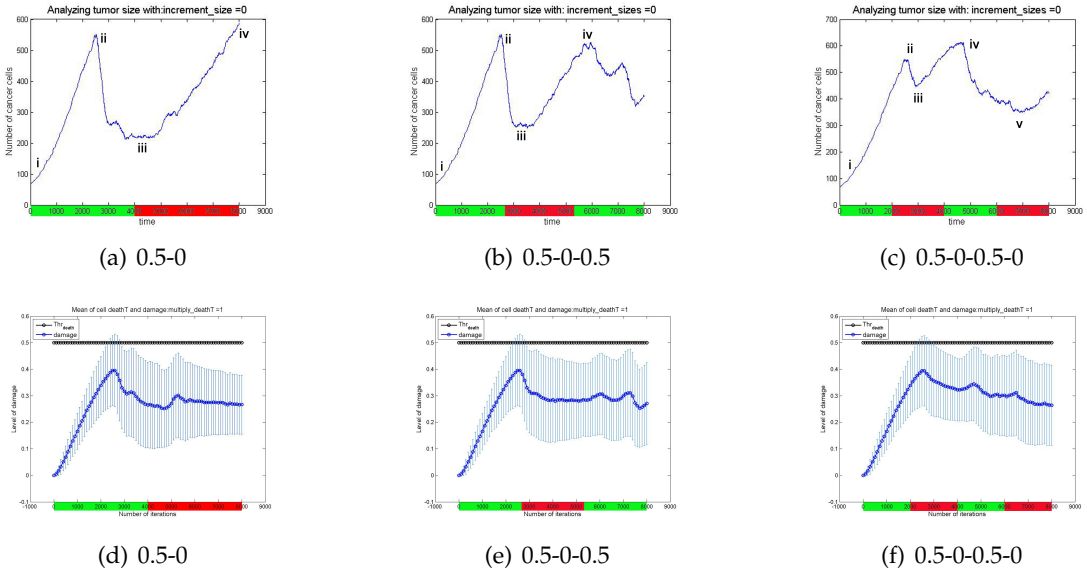

(a) 0.5-0 (b) 0.5-0-0.5 (c) 0.5-0-0.5-0

(d) 0.5-0 (e) 0.5-0-0.5 (f) 0.5-0-0.5-0

Figure 4.4: $DrugIn = 0.5$ *family, failed treatment.* Cancer cells population dynamics and damage accumulation curves for 0.5-0, 0.5-0-0.5 and 0.5-0-0.5-0 are shown in (a,b,c) and (d,e,f) respectively. (d), (e) and (f) show the mean value of accumulated damage of all cells with vertical lines, representing standard deviation, and an average death threshold of all cancer cells (constant in this case). Drug administration and resting intervals are colored green and red respectively.

with lower dose intensity. And indeed in clinical trials maximum-tolerated dose (MTD) protocols are often used to treat cancer. However, it means also the higher overall toxicity to endure for the patient, and so rather long resting intervals to recover are essential. But again, there is then a risk for the tumor to regrow demolishing the chemotherapy effect. Hence, presently, often the alternative drug administration scheme is used, the so-called chemo-switch (C-S) schedule (MTD chemotherapy followed by the metronomic chemotherapy (MET), a low-dose frequently given therapy).This drug administration protocol is proved to be an effective anti-cancer therapy [46], [32].
As in the successful treatment protocols tumor is eradicated before second drug administration is started (or soon after in case 1.5-0-1.5-0)), it was decided to try reverse C-S therapy by increasing a dose intensity in the second drug administration interval. Performed simulations of this protocol showed no complete tumor eradication, but tumor was shrinked to the very small population. Schedules with 3 fraction turned out to be less effective than those with 4 intervals Figure 4.5.
To sum up, in no-resistance case the simulation results improve with division of treatment time into more fractions. It is a very important observation as taking such a drug protocol will reduce the overall toxicity and benefit the patient's condition. However,

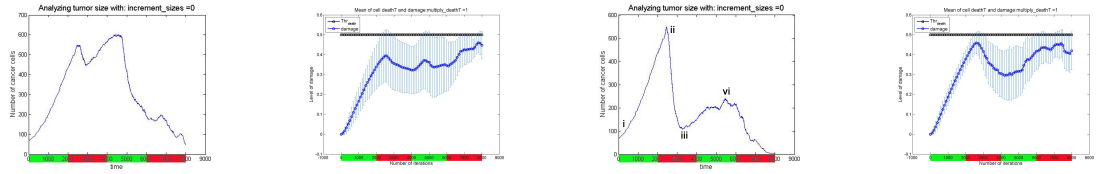

(a) 0.5-0-2-0 (b) 0.5-0-2-0 (c) 1-0-2-0 (d) 1-0-2-0

Figure 4.5: *Increasing dose intensity in second drug administration interval* Cancer cells population dynamics and damage accumulation curves for the drug regimens 0.5-0-2-0 and 1-0-2-0 are shown in (a,c) and (b,d)respectively. (b),(d) show the mean value of accumulated damage of all cells with vertical lines, representing standard deviation, and an average death threshold of all cancer cells (constant in this case). Drug administration and resting intervals are colored green and red respectively.

the choice of the particular drug protocol will depend on one's objective: killing tumor "by all means" as fast as possible or killing tumor, while minimizing total drug amount, does not matter how long it takes. Alternatively one can try to minimize drug exposure time and overall toxicity.
The fastest way to kill the tumor is the 3-0-0 protocol, however, dose intensity and total the toxicity are both high in this case. Better option is to select 2-0-2-0 protocol as the time does not differ that much from 3-0-0 case, but the total toxicity is reduced significantly, the dose intensity stays high though. Compromising some time one can choose 1.5-0-1.5-0 protocol, as the overall amount of drug introduced to the system is lowest for this case. If the objective is to not exceed the $DrugIn = 1$, the case with two fractions 1-0 might be a good option, although the treatment time is relative long and the overall toxicity is slightly higher then that of 1.5-0-1.5-0 case.

4.1.2 Acquired Resistance

Here considered is the case of acquired resistance, when initially no-resistant tumor develop an anti-cancer drug resistance in the course of treatment. The emergence of resistant phenotype can be triggered by the exposure to cytotoxic drug, microenvironment, like intrinsic tumor hypoxia (vasculature geometry), pharmacological sanctuaries that hinder drug diffusion, or other factors [3],[6].
As it was stated in chapter 3 acquired resistance is defined as an individual ability of each cancer cell to increase the level of damage it can withstand if the prolonged drug exposure criterion is met. The death threshold of the cell that is being faced with high drug concentration long enough, will be increased by $increment\_sizes$ parameter. Thus, $increment\_sizes$ value will determine the qualitative behavior of population dynamics. And indeed, as it was revealed in [9] varying $increment\_sizes$ one can observe for $0 \leq increment\_sizes < 3 \times 10^{-5}$ the case of successful treatment, for

$3 \times 10^{-5} \leq increment\_sizes < 4 \times 10^{-5}$ almost successful treatment, for $4 \times 10^{-5} \leq increment\_sizes < 7 \times 10^{-5}$ the emergence of a drug-resistant tumor, $increment\_sizes \geq 7 \times 10^{-5}$ complete treatment failure. Further is considered the impact of different drug administration protocols on the cases of almost successful treatment and the emergence of resistant tumor. The maximum amount of iterations is set to 25000 as it was in [9] and the DNA damage repair remains constant same as for the no resistant case $p = 1.5 \times 10^{-4}$.

Almost successful treatment, increment_sizes 3.5×10^{-5}

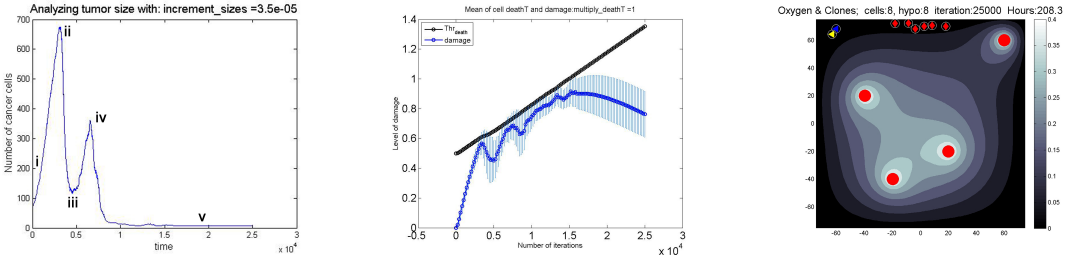

(a) Cancer size (b) Damage curve (c) Remaining cells, iteration 25000

Figure 4.6: *Continuous case*, $increment\_sizes = 3.5 \times 10^{-5}$ Cancer cells population dynamics and damage accumulation curve for the continuous drug supply is shown in (a) and (b) respectively. (c) shows the remaining cells at the end of the treatment course, where the white circles indicate the hypoxic niche. (b) shows the mean value of accumulated damage of all cells with vertical lines, representing standard deviation, and an average death threshold of all cancer cells.

In this subsection analyzed is the impact different drug administration schedules have on the case resulting in almost successful treatment for continuous drug supply. The value for the $increment\_sizes = 3.5 \times 10^{-5}$ parameter was selected from the appropriate range $3 \times 10^{-5} < increment\_sizes < 4 \times 10^{-5}$.
Once again, consider first the case of continuous drug supply DrugIn=1 (Figure 4.6). The cancer cell population dynamics resembles that of no-resistance case with (i-iv) phases. However, starting from iteration 16000, there are only 8 remaining cells located in the hypoxic region (v), which will not proliferate till the end of the treatment course being in quiescent state due to the oxygen deprivation Figure 4.6(c). The hypoxic niche has also low drug concentration resulting in poor drug accumulation by the remaining cells, they are still perform DNA repair though. Thus, the average damage level curve decreases, while, thanks to the acquiring resistance, the average death threshold curve increases.
Following the same logic as in the no-resistance case, the overall amount of drug con-

DrugIn \ Intervals	1 D	2 D-0	3 D-0-0	3 D-0-D	4 D-0-D-0
0.5		934 8		939 8	941 8
1	8 3	8 3		840 2	944 1
1.5		0 7525 45150 0		0 7525 45150 0	0 7525 37500 0
2		0 4732 37856 0			0 4732 37856 0
3			0 4595 55140 0		

Table 4.2: *Acquired resistance* ($increment\_sizes = 3.5 \times 10^{-5}$). The cases of successful tumor eradication and cases with overall amount of drug lesser than 100000 are marked with green background color and blue font color respectively. Table entries: number of survived cells, number of iterations (omitted in case of failed treatment), overall amount of drug (omitted in case of failed treatment), number of survived clones.

tinuously supplied to the system $25000 \times 4 \times 1 = 100000$, was taken as an upper bound for the different drug protocols. The simulation results for different treatment regimens are presented in Table 4.2. The drug administration regimens with $DrugIn > 1$ achieved a complete cancer response to the treatment. Although, in these cases it has required more time for the tumor eradication, the cell evolution curves and damage plots are rather similar to those of no-resistance case Figure 4.2. The tumor dynamics shows only two phases (i-ii): cells that still have not encountered enough drug will increase the population size and then die out due to the accumulated damage.
Now, consider "families" of the failed treatment cases: $DrugIn = 1$ and $DrugIn = 0.5$. Just as it was observed in the case of no-resistance, also in case of acquired resistance 1-0 protocol duplicates the outcome for continuous drug supply (see Figure 4.6) with its partial treatment response. 1-0 regimen shows 8 persistent cancer cells stuck in the hypoxic region at the end of the treatment, however, now, this result is obtained using 50000 units of drug lesser.
1-0-1 and 1-0-1-0 in their turn are examples of resistant tumor taking over the domain. In 1-0-1 protocol two periods of tumor shrinkage are followed by tumor expansion Figure 4.7 (a). In the phase (v) there are only 8 cells remained, however, unlike the

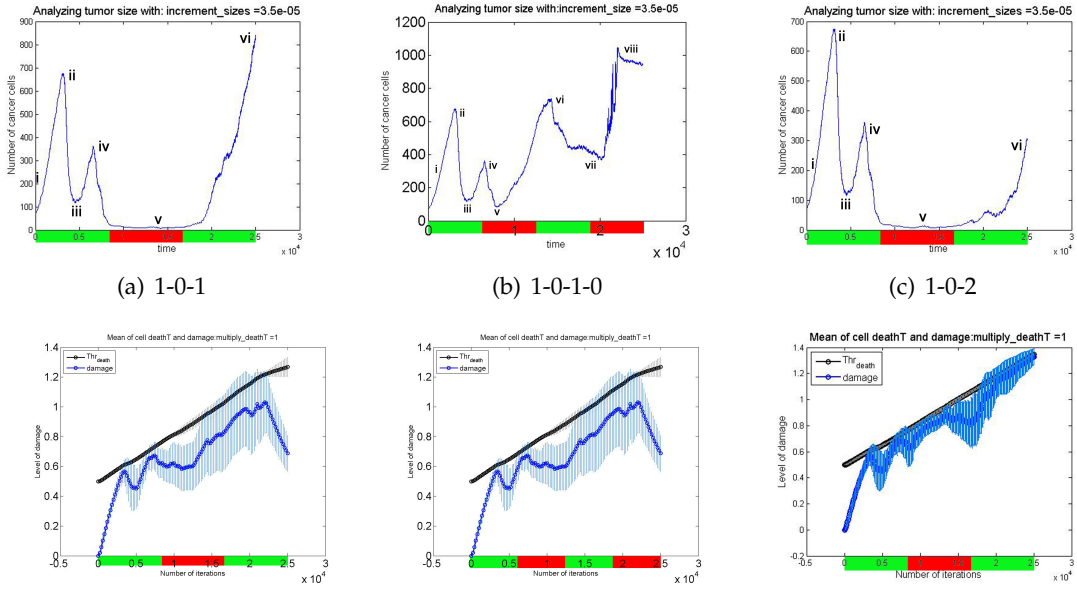

(a) 1-0-1 (b) 1-0-1-0 (c) 1-0-2

(d) 1-0-1 (e) 1-0-1-0 (f) 1-0-2

Figure 4.7: $DrugIn = 1$-*family*, $increment\_sizes = 3.5 \times 10^{-5}$ Cancer cells population dynamics and damage accumulation curve for the continuous drug supply is shown in (a),(b),(c) and (d),(e),(f) respectively. (d),(e),(f) show the mean value of accumulated damage of all cells with vertical lines, representing standard deviation, and an average death threshold of all cancer cells.Drug administration and resting intervals are colored green and red respectively.

continuous case, due to the low amount of cells in the domain, level of oxygen has increased and reached the hypoxic cells, thus allowing them to proliferate again. During the resting interval, drug is being washed out of the domain(sink boundary conditions) and taken up by the persistent cells. Thus, cells receive minor damage, while repairing their DNA and acquiring resistance Figure 4.7 (b). As follows, they became unresponsive to the drug what resulted in disease progression. In case of 1-0-1-0 regimen, cells escape repeatedly to the low drug normoxic niche, which allows them to keep tumor population from extinction and ensure the cancer expansion. Due to the intervals shortening there is not enough time to kill off the tumor, while drug is administrated, but sufficient for it regrow in the resting intervals.

Next, considered is $DrugIn = 0.5$-family of schedules Figure 4.8. One can observe a complete treatment failure. Prolonged exposure to the low drug doses allows tumor cells increase of death threshold accompanied by easy DNA repair. In case of 0.5-0, common tumor behavior prior to damage accumulation (i-ii) is followed by rather peculiar one in the low drug niche (iii), showing small fluctuations of the cell population size. As long as drug is administrated slight increase of cell amount will be eradicated not allowing tumor expansion. But soon after resting interval starts, some cells are still

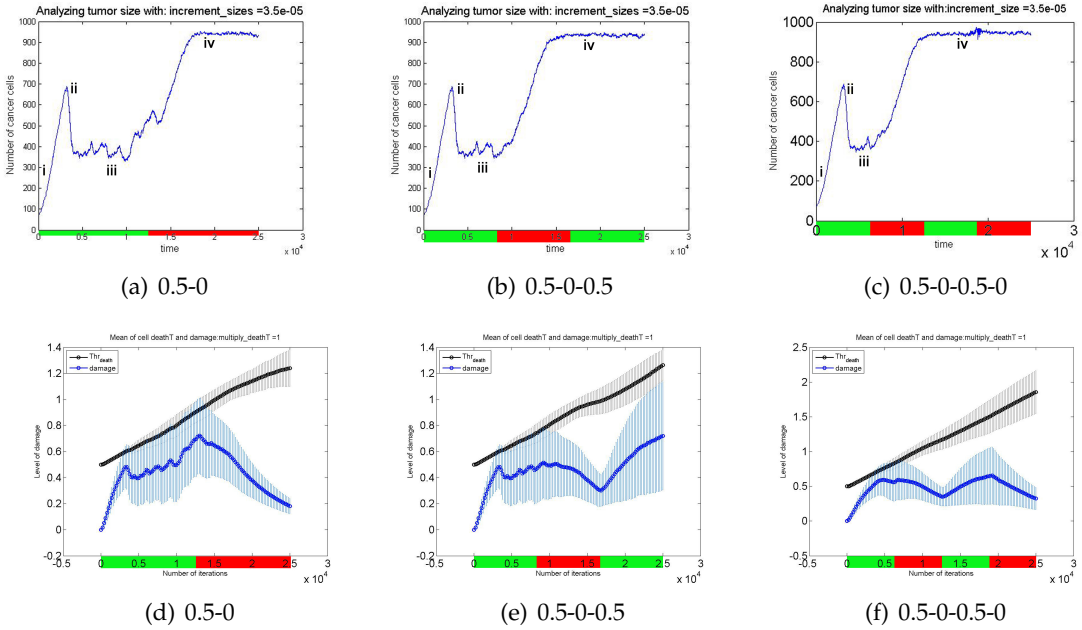

(a) 0.5-0 (b) 0.5-0-0.5 (c) 0.5-0-0.5-0

(d) 0.5-0 (e) 0.5-0-0.5 (f) 0.5-0-0.5-0

Figure 4.8: $DrugIn = 0.5$-*family*, $increment\_sizes = 3.5 \times 10^{-5}$ Cancer cells population dynamics and damage accumulation curve for the continuous drug supply is shown in (a),(b),(c) and (d),(e),(f) respectively. (d),(e),(f) show the mean value of accumulated damage of all cells with vertical lines, representing standard deviation, and an average death threshold of all cancer cells.Drug administration and resting intervals are colored green and red respectively.

killed due to the residual drug but then tumor take over the domain. 0.5-0-0.5 shows same behavior with only difference phase (iii) being shorter. The division into 4 intervals shows the worst outcome as tumor expansion starts much earlier.
Once again in effort to improve results, protocols with mixed dose intensities were tried, but to no avail. Outcomes of the application of higher dosage in the second drug administration interval for $DrugIn = 0.5$ and 1 failed cases mostly have duplicated the original results. Thus, dose intensity of the first drug administration interval seems to have more influence on the final outcome. Protocols with 3 fractions performed better then those with 4 intervals. As in case of 4 fractions at the time point when higher dose is administrated most of the cancer cells have already acquired resistance, hence, unresponsive to the therapy. The most significant change showed 1-0-2 schedule shrinking tumor size compared to 1-0-1 from 840 to 306 cells Figure 4.7(c)(vi). Moreover, remaining cancer cells suffering high level of damage Figure 4.7(f), thus, might eventually die out.
To conclude, in case of acquired resistance with $increment\_sizes 3.5 \times 10^{-5}$ the fastest tumor eradication can be observed for 3-0-0 protocol. However, the overall toxicity burden as well as drug dosage is high. Thus, it would be reasonable therefore to choose one

of the $DrugIn = 2$ regimens. These schedules require just about 100 iterations more to kill off the tumor, yet toxicity level is reduced in almost 1.5 times. $DrugIn = 1.5$ turned out to be less effective than $DrugIn = 2$ needing more time to eradicate tumor with rather high toxicity level.

Emergence of drug resistance, increment_sizes 4.5×10^{-5}

The case of emergence of drug resistance can be characterized with reduced anti-cancer drug efficacy in the long-term. The differences in cancer population behavioral patterns for this case are determined by the choice of $increment\_sizes$ parameter value. The higher value is, the higher is the average death threshold, thus the more resistant are the cells, leading eventually to the complete treatment failure case. Here is considered the case with $increment\_sizes = 4.5 \times 10^{-5}$, which shows rather promising results on the onset of the treatment course, but end up with expansion of resistant tumor in the domain. Simulation results are presented in Table 4.3.

One should note here that tumor population dynamics in onset of the treatment for

DrugIn \ Intervals	1 D	2 D-0	3 D-0-0	3 D-0-D	4 D-0-D-0
0.5		932 8		945 9	952 11
1	935 1	930 1		935 1	935 1
1.5		327 1		346 1	323 1
2		1 1			1 1
3			0 5335 64020 0		

Table 4.3: *Acquired resistance* ($increment\_sizes = 4.5 \times 10^{-5}$). The cases of successful tumor eradication and cases with overall amount of drug lesser than 100000 are marked with green background color and blue font color respectively. Table entries: number of survived cells, number of iterations (omitted in case of failed treatment), overall amount of drug (omitted in case of failed treatment), number of survived clones.

all $DrugIn > 1$ protocols follows two phases behavior Figure 4.2 (a), common for all successful treatment cases. However, complete tumor eradication can be observed only for 3-0-0 protocol. $DrugIn = 2$-family of schedules also manages to almost kill off the tumor, but fails in the end. In Figure 4.9(a) is illustrated cell population dynamics exam-

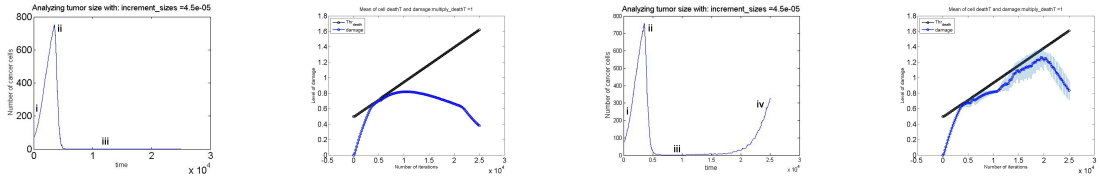

(a) $DrugIn = 2$ (b) $DrugIn = 2$ (c) $DrugIn = 1.5$ (d) $DrugIn = 1.5$

Figure 4.9: $DrugIn > 1$ *plots* $increment\_sizes = 4.5 \times 10^{-5}$ Cancer cells population dynamics and damage accumulation curves are shown in (a),(c) and (b),(d) respectively. (b),(d) show the mean value of accumulated damage of all cells with vertical lines, representing standard deviation, and an average death threshold of all cancer cells.

ined in both $DrugIn = 2$ protocols. After iteration 5400, there is only one cell remains that can not be eradicated being in low drug hypoxic niche. Due to vasculature geometry it suffers strong oxygen deprivation. Even after oxygen, owing to absence of other cells, restores its healthy tissue gradient Figure 3.2(a) the persistent cell continues being hypoxic. Albeit, this case can be considered as successful tumor suppression, Figure 4.9 (b) shows that remaining cell is resistant. Hence if it manages to re-enter the cell cycle, it won't respond to the treatment, as it was observed in $DrugIn = 1.5$ case Figure 4.9 (c). For $DrugIn = 1.5$ protocols, after iteration 6400 there are two persistent cells in low drug region that switch to quiescent state, being deprived of oxygen. However, thanks to the fortunate cells' location eventually they managed to start proliferation process again, as oxygen level had increased. This cancer cell population is unresponsive to the therapy causing disease progression and further treatment complications.

Next is considered $DrugIn = 1$-family of drug schedules Figure 4.10. Continuous case as well as 1-0 case shows two periods of cancer cell repopulation (i-iv) followed by the tumor shrinkage (v) to 27 cells and further disease progression (vi). This survived cell subpopulation (v) is located in the low drug niche, thus drug level is not enough to kill off tumor completely. This accompanied with steady DNA repair and death threshold increase results in resistant tumor expansion, where in case 1-0 tumor is much more resistant. Figure 4.10 (b),(c) show that dividing treatment time into more fractions results in shortening of tumor shrinkage period as well as increasing of the amount of survived cells in (v). In case 1-0-1, during resting interval, after increasing its size in (iv), cell population size still decreases due to the sufficient amount of residual drug in the domain. Whereas in case of 1-0-1-0 protocol tumor size attained in (iv) is poorly affected in (v), as tissue slice failed to accumulate enough drug. All $DrugIn = 1$-regimens lead to the resistant tumor, which takes over the domain.

Cancer behavior, while being treated with $DrugIn = 0.5$ protocols ended up being quite similar to the one for $DrugIn = 1$. There are two cancer grow periods with local population size minimum at (v). Difference is that the local minimum at (v) attained by $DrugIn = 0.5$ protocols is much higher than for $DrugIn = 1$, as low drug dosage

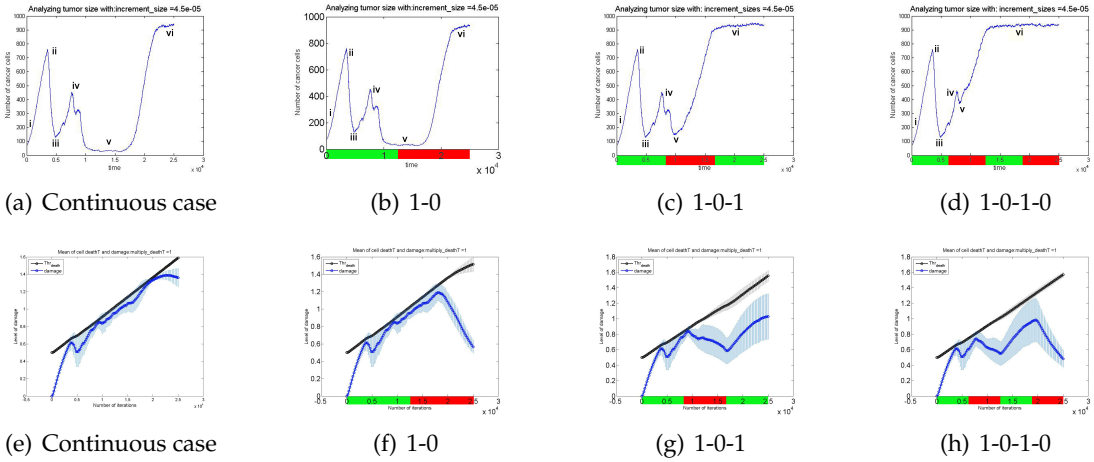

(a) Continuous case (b) 1-0 (c) 1-0-1 (d) 1-0-1-0

(e) Continuous case (f) 1-0 (g) 1-0-1 (h) 1-0-1-0

Figure 4.10: $DrugIn = 1$-*family*, $increment\_sizes = 4.5 \times 10^{-5}$ Cancer cells population dynamics and damage accumulation curves are shown in (a),(b),(c) and (d),(e),(f),(g) respectively. (d),(e),(f),(g) show the mean value of accumulated damage of all cells with vertical lines, representing standard deviation, and an average death threshold of all cancer cells.Drug administration and resting intervals are colored green and red respectively.

is less effective against cancer. In case of 0.5-0-0.5-0 similarly to 1-0-1-0 (iv-v) phases almost completely disappear, presenting the resistant tumor.
Based on the analysis of previous cases, one of major causes of cancer expansion is tumor repopulation during the drug pause interval. Thus, in order to shorten resting time, 5 fractions protocol was introduced $DrugIn = 1\frac{2}{3} \approx 1.67$. The observed behavior replicates that for $DrugIn = 2$ cases with one persistent cell in the hypoxic niche Figure 4.9 (a),(b).
Applying chemo-switch regimen, administrating lower drug dose after the higher one haven't affected population behavior. Same should be mentioned for the reverse chemo-switch, with higher dose on the second active therapy interval. This once again proves the crucial impact dose intensity of the first drug administration interval has on the further disease development.
To sum up, the best treatment protocol and the only successful one is 3-0-0, however, the overall toxicity is high. One may decide on 2-0-2-0 protocol and just terminate drug supply soon after 5400 iteration. However in this case there is a possibility of disease relapse.

Emergence of drug resistance, increment_sizes 5.9×10^{-5}

Similarly to $increment\_sizes = 4.5 \times 10^{-5}$, this case also illustrates reduced effectivity of the drug as the time advances, resulting in tumor population that is not responding to the treatment. However, now, acquiring resistance, due to the high $increment\_sizes$

value, takes much less time. The simulations outcomes are summarized in Table 4.4.
There is no successful treatment protocol observed this time. Moreover, cancer cell

DrugIn \ Intervals	1 D	2 D-0	3 D-0-0	3 D-0-D	4 D-0-D-0
0.5		934 15		941 15	934 26
1	942 4	927 4		943 6	967 6
1.5		938 15		936 12	930 14
2		935 9			933 8
3			937 15		

Table 4.4: *Acquired resistance* ($increment\_sizes = 5.9 \times 10^{-5}$). The cases of successful tumor eradication and cases with overall amount of drug lesser than 100000 are marked with green background color and blue font color respectively. Table entries: number of survived cells, number of iterations (omitted in case of failed treatment), overall amount of drug (omitted in case of failed treatment), number of survived clones.

population dynamics for all drug schedules follows the same behavioral pattern: increasing in the beginning of treatment course(i), attaining its local maximum(ii), dying due to the accumulated damage and reaching local minimum(iii) and then starting to repopulate the domain not responding to the drug anymore. However, it still differs in its max and min values depending on the dose intensity Figure 4.11. Where schedules with doses $DrugIn > 1$ reduce tumor size to the lowest minimum value.
Introduction of more fractions to shorten resting time, won't benefit treatment response in case of $increment\_sizes = 5.9 \times 10^{-5}$. 5 fractions schedule with $DrugIn = 1.67$ showed results similar to $DrugIn = 1.5$ cases allowing resistant tumor expansion as well Figure 4.11 (c),(f). Dividing treatment time into 10 intervals ($DrugIn = 2$), resulted into complete treatment failure, with cancer population behavior similar to Figure 4.11 (a),(d). Similarly as it was the case in previously examined $increment\_sizes = 4.5 \times 10^{-5}$, applying different dosages in treatment course will not influence treatment outcome.
In case of $increment\_sizes = 5.9 \times 10^{-5}$ simulations show complete treatment failure with evident drug resistance for all observed drug administration regimens. Thus, the best treatment strategy would be to refrain from high dose intensities as they lead to the tumor heterogeneity.
In conclusion, treatment schedules with higher dose, with exception of $increment\_sizes = 5.9 \times 10^{-5}$ case, showed better treatment outcomes. This complies with conventional chemotherapeutic treatment using maximum tolerated dose. Whereas, reduction of

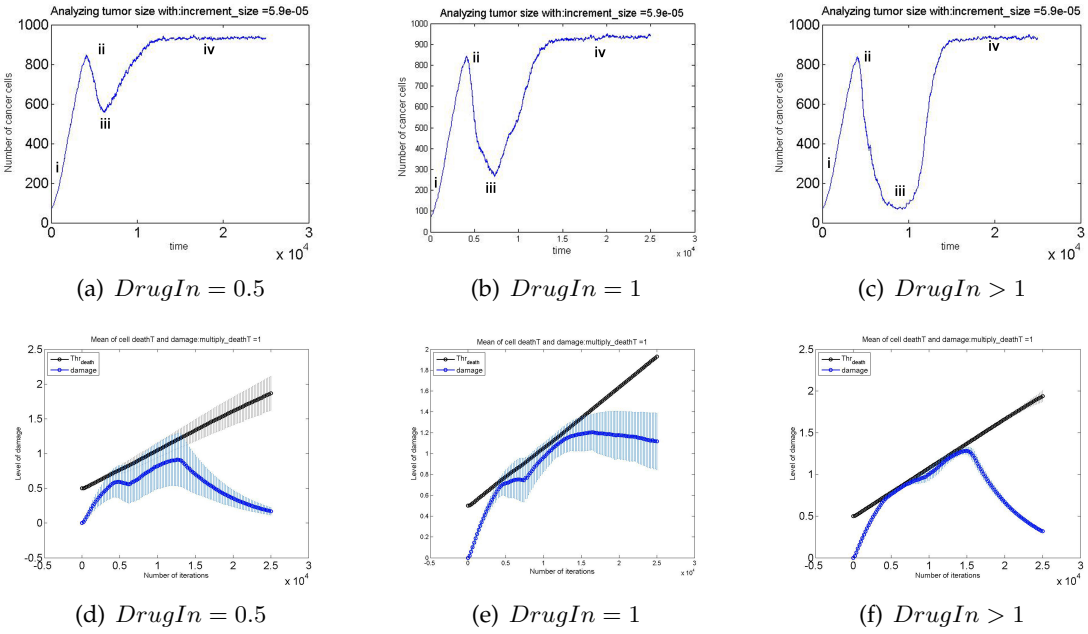

(a) $DrugIn = 0.5$ (b) $DrugIn = 1$ (c) $DrugIn > 1$

(d) $DrugIn = 0.5$ (e) $DrugIn = 1$ (f) $DrugIn > 1$

Figure 4.11: *Population size and damage accumulation curves,* $increment\_sizes = 5.9 \times 10^{-5}$ Cancer cells population dynamics for different dose intensities is shown in (a), (b), (c). (d),(e) and (f) show the mean value of accumulated damage of all cells with vertical lines, representing standard deviation, and an average death threshold of all cancer cells.

dose intensity below the value, determined through the model calibration ($DrugIn = 1$), appeared to be less effective resulting in expansion of resistant tumor. Application of drug schedules combining different doses showed little improvement, due to the impact the first drug administration interval has on the disease development.
Introducing resting intervals proved to be a good method to reduce overall toxicity, which will improve patient's condition. However, long breaks between drug administration intervals allow cancer cell population to regrow and develop resistance. Whereas, shortening of drug pauses in between active therapy for some dose intensities may lead to the strongly heterogeneous tumor that will eventually not respond to chemotherapy. Analysis of treatment protocols in this subsection was made based on their efficacy in tumor eradication, whereas the next one observe them from the clonal perspective.

4.2 Tumor clonal evolution analysis

In this subsection is analyzed the impact of different drug administration regimens on the clonal diversity of tumor. This issue is investigated by the means of phylogenetic trees showing the tumor clonal evolution. The model used in this thesis gives the op-

portunity to track life history of each individual cell. The tree graph shows all remaining cells at the last iteration as leaves, cells' mothers as nodes and the initiating cell as the root.
The analysis of different drug protocols in section 4.1 has revealed that some failed therapies result in increasing tumor heterogeneity. In this section is investigated what is rather to cause clonal diversity: dose intensity or introduction of resting intervals between drug administration.

4.2.1 No resistance

First of all, consider survived clones in the no-resistance case Table 4.1. For the failed treatment regimens with $DrugIn = 1$, there is only one survived clone. Thus tumor heterogeneity in these cases is caused by the introducing of resting intervals, which allow cancer cell repopulation. The observations in both cases are quite similar, the clone wasn't eradicated due to the favorable spatial location of the initial cell. Clonal subpopulation has managed to outcompete other clones as it was located in the low drug niche. In Figure 4.12 (i) there are 3 clones left, where two phenotypes are at disadvantage being located in the hypoxic region. (ii), (iii) show yellow and blue diamonds being thrown out of the domain with red diamond phenotype spread out in the tissue. The inheritance tree for the 1-0-1 protocol is presented in Figure 4.12(c). One can see the long division history of the clone, as its initiating cell was located in the low drug normoxic region and was able to proliferate throughout the treatment course. As for

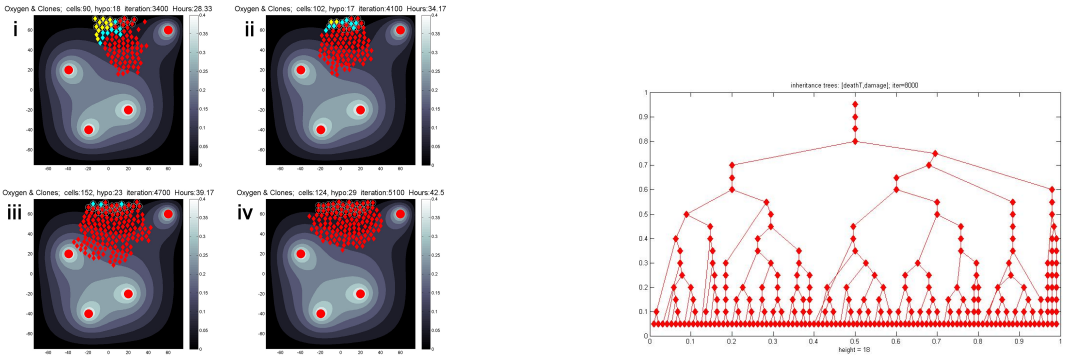

(a) (b)

Figure 4.12: *No-resistance case (1-0-1), clonal evolution* The snapshots (a) and (b) show the location of the survived clone. In (c) the inheritance tree is presented.

the $DrugIn = 0.5$-family of drug administration regimens, the survival of cell clones can be explained by the low dose intensity. The insufficient effect of the observed drug concentration enables tumor to preserve its clonal diversity. After first interval of drug administration in case of 0.5-0 protocol, the amount of distinct clones is 18, for 0.5-0-0.5 it is 58. Those clones that are located in hypoxic or low drug niches, will proliferate and

overtake a large part of domain.
The situation for the 0.5-0-0.5-0 protocol is even more problematic as the beginning of

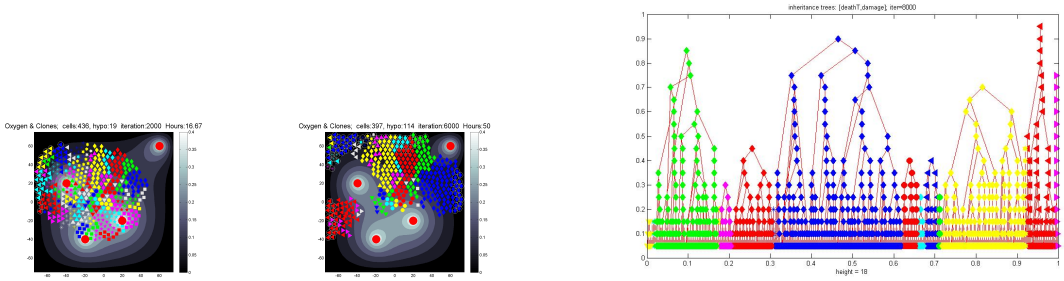

(a) (b) (c)

Figure 4.13: *No-resistance case (0.5-0-0.5-0), clonal evolution* The snapshots (a) and (b) show the clonal diversity at iteration 2000 and 6000 respectively. In (c) the inheritance tree is presented.

the first resting interval coinside with the phase of active cancer cells proliferation, as they still haven't got enough damage to exceed the death threshold Figure 4.13. Thus all the 65 initial clones are still present Figure 4.13(a). At the end of the second drug administration interval (iteration 6000 Figure 4.13(b)) there are still 32 clones located in the low drug niches. One can observe in the phylogenetic tree that the cells, which were located in the hypoxic regions, have shorter life history, as they remained in the quiescent state. Whereas, those whose initial cell was located near low drug and haven't suffered oxygen deprivation have divided more often.

4.2.2 Aquired resistance

Next, consider the acquired resistance case. Based on the $increment\_sizes$ parameter one can observe quite different scenarios, where due to cell's ability to acquire resistance, tumor clonal diversity got much more affected by the choice of particular drug administration protocol.

$increment\_sizes = 3.5 \times 10^{-5}$

As it was mentioned in subsection 4.1.2, 1-0 drug protocol duplicates the result for continuous drug supply case. The 8 surviving cells starting from iteration 11700 are stuck in the low drug hypoxic niche in resting state not able to proliferate. The initiating cells of these surviving phenotypes were located near the pharmacological sanctuaries, thus, allowing them to escape death in hypoxic regions.
The daughter tree report Figure 4.14(b) shows a short cell fate, because 3 presented

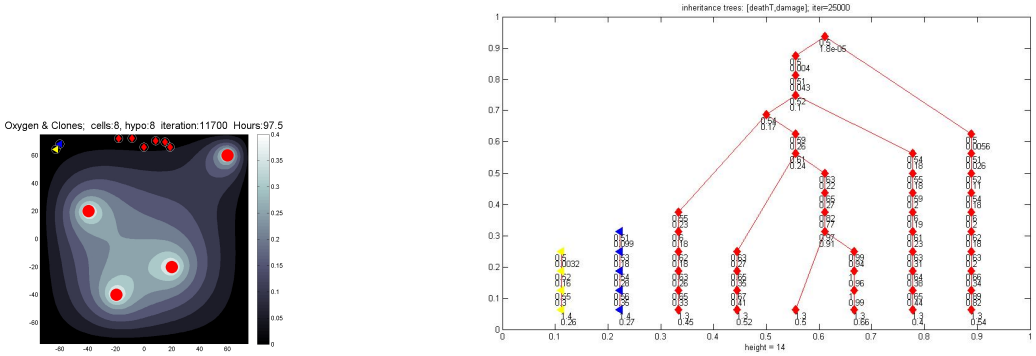

(a) (b)

Figure 4.14: $increment\_sizes = 3.5 \times 10^{-5}$ *(1-0), clonal evolution* In (a) the remaining clones stuck in the hypoxic region are shown. (b) shows the inheritance tree with values for death threshold and damage.

clones became quiescent already in the first part of the treatment course. At the same time cells have been repairing their DNA and increasing death their threshold, becoming resistant.

The 1-0-1 protocol resulted in interesting outcome that gives the situation, described above, a new twist by allowing one of the persistent clones to re-enter the cell cycle Figure 4.15. As the domain has no other cells to consume oxygen it leads to an increased oxygen supply to hypoxic regions, thus trigger the proliferation of one of the clones. In clinical trials it is often the case that during the resting interval between drug administration cancer cell repopulation takes place. When the drug is administrated again, the cells, due to the acquired resistance, do not respond to treatment anymore.

The clone that started the tumor expansion, increases its subpopulation size and

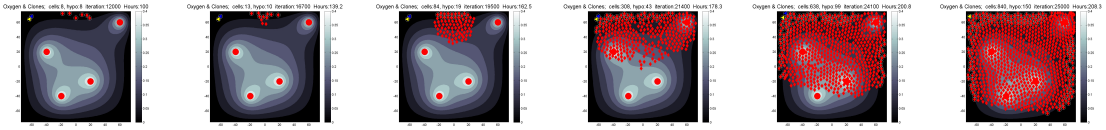

(a) (b) (c) (d) (e) (f)

Figure 4.15: $increment\_sizes = 3.5 \times 10^{-5}$ *(1-0-1), clonal evolution* The process of tumor expansion by a persistent clone.

"throws" blue triangle cell phenotype out of the domain. The 1-0-1-0 protocol differs only by the fact that the persistent clone manages to get rid of both other clones being the only survivor at the of the treatment course.

The family of $DrugIn = 0.5$ regimens showed uniform simulation outcomes. At the end of each treatment protocol there are 8 remaining clones in the domain Figure 4.16.

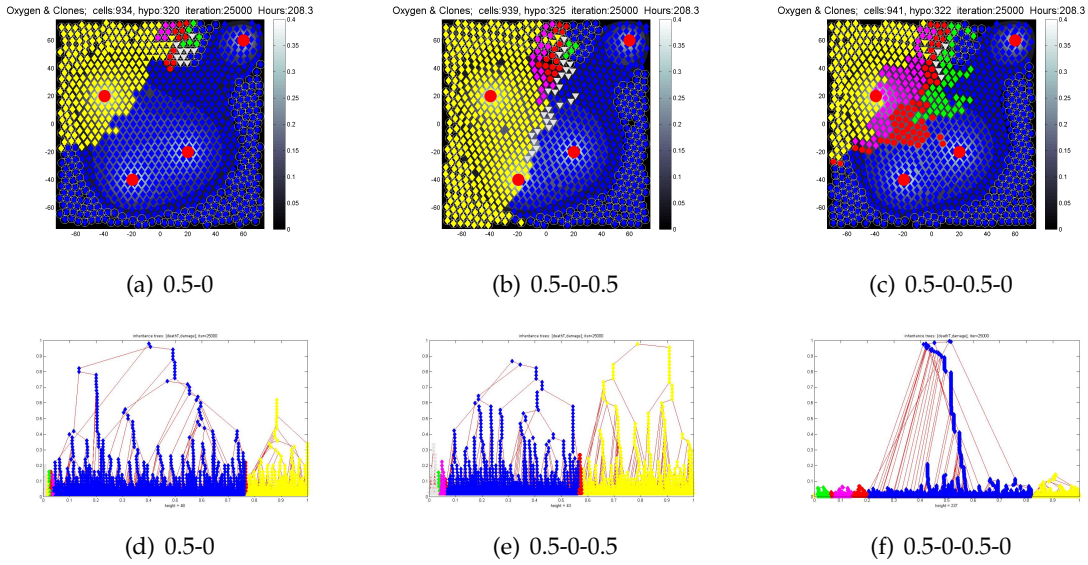

(a) 0.5-0 (b) 0.5-0-0.5 (c) 0.5-0-0.5-0

(d) 0.5-0 (e) 0.5-0-0.5 (f) 0.5-0-0.5-0

Figure 4.16: $increment\_sizes = 3.5 \times 10^{-5}$ *($DrugIn = 0.5$-family), final clonal configuration* The dependence of quantitative ratio of clonal subpopulation on a drug administration regimen.

Similarly to the case of no resistance, drug concentration is too low to inhibit the cell growth. However, the amount of cells of each phenotype differs in these cases. This can be explained with different time point and duration of the resting intervals, allowing repopulation for those clones that have the most favorable environmental conditions at this moment.
Figure 4.16 (d,e,f) show the phylogenetic trees of the $DrugIn = 0.5$ protocols. The longest cell life histories have blue and yellow "diamonds". Their initiating cells are located near the low drug niche, thus allowing them to increase their subpopulations. Yet, in 0.5-0-0.5-0, only the blue clone was able to divide freely, while the yellow one had to compete with other cell clones, which were regrowing due to early resting interval.

$increment\_sizes = 4.5 \times 10^{-5}$

For both protocols of $DrugIn = 2$-family, cells dynamics simulation outcome can be described as follows: starting from iteration 5400 there is only one survived hypoxic cell, which is located in the strongly hypoxic region, thus absolutely deprived of oxygen supply Figure 4.17(a)(i). Even after increase of average oxygen concentration in the domain (ii), this clone still fails to receive enough nutrient to re-enter the cell cycle.
Consider protocol 1.5-0, there are 2 clones at iteration 5500 represented by 6 hypoxic cells, later, at iteration 6400, only 1 clone with 2 cells remains Figure 4.17(b). The reason why yellow diamond phenotype goes extinct is high damage level accumulated by the cells. Whereas DNA damage burden carried by blue diamonds is lesser and after repair

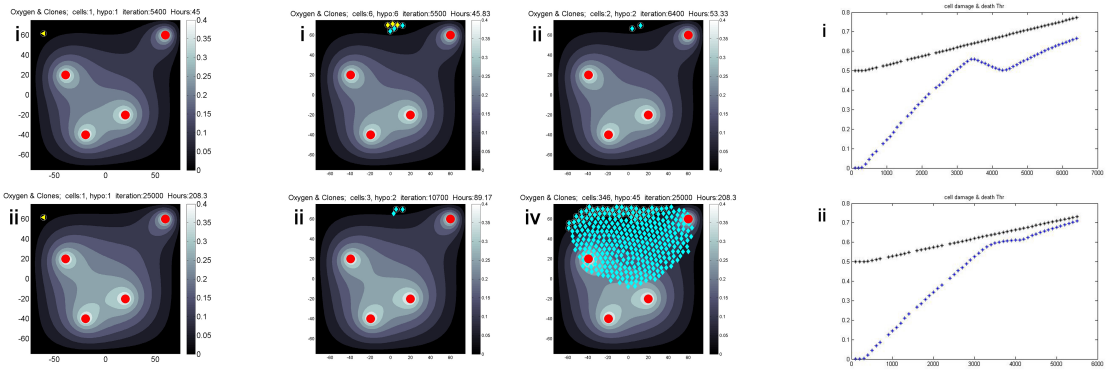

(a) $DrugIn = 2$ (b) $DrugIn = 1.5$ (c) Damage curves

Figure 4.17: $increment\_sizes = 4.5 \times 10^{-5}$ *(2-0; 1.5-0), clonal evolution* 2-0 protocol result with remaining cell stuck in the hypoxic region is shown in (a). (b) illustrates the process of tumor expansion by a persistent clone in case of 1.5-0 regimen. (c) shows damage curves of the two cells at the iteration 6400 (b)[ii]

at 6400 decreases further. At iteration 10700 blue diamond phenotype representatives build therapy resistant cancer due to the acquired resistance Figure 4.17(c). Empty domain with no cells to uptake the oxygen, allows its concentration increase, and hence reoxygenation of hypoxic cells. It enables for a hypoxic clone to divide at 10700 and thus start cancer expansion. As for other protocols of $DrugIn = 1.5$-family, further division into fractions won't affect clonal diversity, but rather amount of surviving cells.

Consider regimens with $DrugIn = 1$ Figure 4.18. In the course of treatment, when

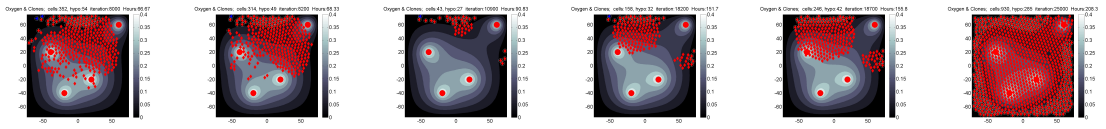

(a) (b) (c) (d) (e) (f)

Figure 4.18: $increment\_sizes = 4.5 \times 10^{-5}$ *(1-0), clonal evolution* The process of tumor expansion by a persistent clone.

drug concentration is increasing, tumor is shrinked to the small population in hypoxic regions with 2 clones (one of them not completely quiescent). As a result of lessened amount of cells in the domain, oxygen level rise, whereas drug concentration is reduced (no drug supply, cellular uptake and sink boundary conditions). Meantime cells are repairing their DNA and increasing death threshold, hence, when active clone starts to repopulate domain, it is already resistant to the medication. The other clone remains hypoxic, until it is thrown outside the boundary, due to the overcrowding. The division

into fraction does not affect clonal diversity but only the amount of cells present after the treatment course.
The behavior of cancer cell population being treated with $DrugIn = 0.5$ protocols is highly influenced by the low drug concentration. Due to the drug accumulation in tissue, in case of 0.5-0, more distinct clones are killed, whereas in the last case (0.5-0-0.5-0) due to the only short exposure to the low drug dose , DNA repair and acquired resistance more clones managed to survive. The cell division history depends on the initial cell location - microenvironmental niches are more favorable for proliferation.

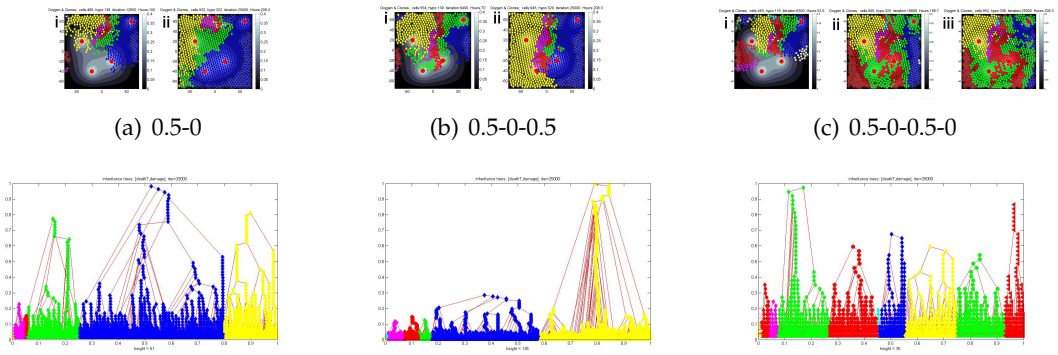

(a) 0.5-0 (b) 0.5-0-0.5 (c) 0.5-0-0.5-0

(d) 0.5-0 (e) 0.5-0-0.5 (f) 0.5-0-0.5-0

Figure 4.19: *Clonal evolution*, $increment\_sizes = 4.5 \times 10^{-5}$, $DrugIn = 0.5$ (a),(b),(c) show clonal configuration at the end of drug administrating interval and at the end of the treatment. (d),(e),(f) show phylogenetic trees.

Figure 4.19 shows remaining clones after active drug therapy. However, this number will be reduced in the further iterations, as some of clones eventually die due out to the accumulated damage while the other ones, presented by small subpopulations located in hypoxic niches (not proliferating), will be thrown out of the domain due to the overcrowding, caused by dividing cell phenotypes located in low drug regions. The daughter cell tree for 0.5-0 shows long cell history for the 3 clones with largest subpopulations, the proliferation process of other ones was suppressed because of the overcrowding. In case of 0.5-0-0.5 schedule, after first drug administration interval, the most advantageous locations, with free space to proliferate, have yellow and blue diamond phenotypes, whereas other clones are squeezed inbetween. Nevertheless, as it is visible on the phylogenetic tree, the blue diamond subpopulation has activated its proliferation only at the conclusion of the treatment, being most of the time partially hypoxic or lacking space to divide. The 0.5-0-0.5-0 protocol with its low drug concentration and short drug administration time allows survival of 21 clones after first interval. However, due to the accumulated damage and competing for space the amount of clones will decrease. As $increment\_sizes$ value is relatively high the role of microenvironmetal niche in selecting the surviving phenotypes is reduced. Therefore, not all of

the persistent clones originate from the same low-drug normoxic region.
To sum up, apart from heterogeneity that is caused by the low dose intensity, dividing treatment time into fractions will only increase tumor clonal diversity.

$increment\_sizes = 5.9 \times 10^{-5}$

When the death threshold increment parameter value equals $increment\_sizes = 5.9 \times 10^{-5}$ the treatment results in disease progression with resistant heterogeneous tumor taking over the tissue slice.
Considering the numerical simulations already the continuous case shows 4 persistent clones in the end of the treatment course. What is more surprising is that the therapy with the high drug dose intensities $DrugIn > 1$ caused tumor to become even more heterogeneous than in $DrugIn = 1$. As it is the case in clinical trials, cancer treated with high dose chemotherapy if not eradicated completely will develop resistance and thus result in much more dangerous malignancies.
After active drug administration in 3-0-0 protocol there are 30 distinct cell phenotypes

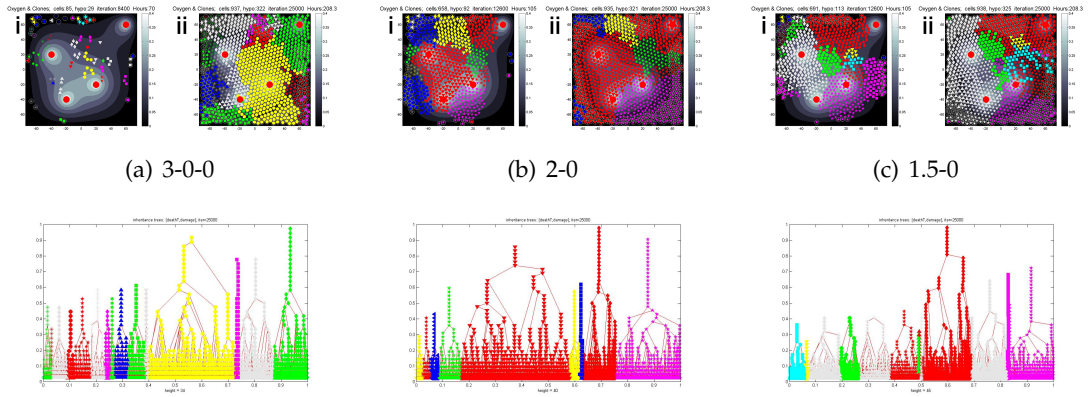

(a) 3-0-0 (b) 2-0 (c) 1.5-0

(d) 3-0-0 (e) 2-0 (f) 1.5-0

Figure 4.20: *Clonal evolution*, $increment\_sizes = 5.9 \times 10^{-5}$, $DrugIn > 1$ (a),(b),(c) show clonal configuration at the end of drug administrating interval and at the end of the treatment. (d),(e),(f) show phylogenetic trees.

left located all over the tissue slice . The clones positioned in the low-drug normoxic niche being sufficiently oxygenated have better conditions to spread out, whereas those being quiescent will be eventually thrown out of the domain by the actively proliferating clones.The situation for other high dose regimens is rather similar. The phylogenetic show approximately same cell life history length for the most of the clones, with the exception of being longer for the domineering phenotypes. This can be explained by the overcrowding condition in the domain when the proliferation process is suppressed until there are free space to divide. Figure 4.20

For $DrugIn = 1$ protocols Figure 4.21 the amount of cells in tumor increases with the

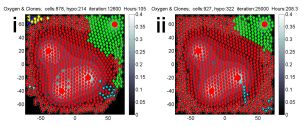

(a) 1-0

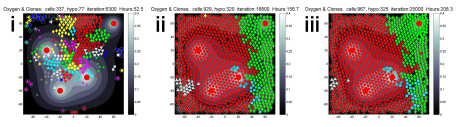

(b) 1-0-1-0

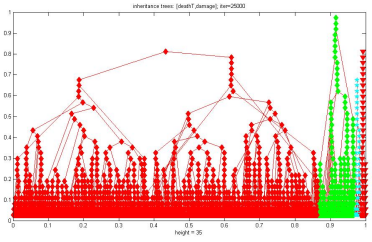

(c) 1-0

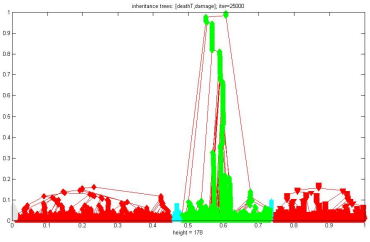

(d) 1-0-1-0

Figure 4.21: *Clonal evolution*, $increment\_sizes = 5.9 \times 10^{-5}$, $DrugIn = 1$ (a),(c) show clonal configuration at the end of drug administrating interval and at the end of the treatment. (b),(d) show phylogenetic trees.

number of fractions showing the highest quantity (967 cells) for the 4 intervals regimen. As for the clonal diversity,it was rather low for all $DrugIn = 1$ regimens. For 1-0 schedule, just as for continuous case, the final tumor configuration shows malignancy composed out of 4 clones, with one being the domineering one. All the persistent clones originated from the cells located in low-drug normoxic niche. 1-0-1 and 1-0-1-0 show quite similar result with 6 clones tumor. Green diamond cell phenotype in 1-0-1-0 also originated from low-drug normoxic region cell remaining in this favorable location throughout the treatment, hence, actively proliferating, which could be observed in its long cell life history.

$DrugIn = 0.5$-family's performance Figure 4.22 was rather disappointing with 0.5-0-0.5-0 protocol showing the worst result out all simulations presented in this thesis leading to very heterogeneous tumor composed of 26 clones. Since $increment\_sizes$ value is quite large, acquiring resistance has a strong influence on cells survival. However the micronvironamental niches still play significant role in the final tumor clonal configuration. After first drug administration interval there are cell clones originating from all over the tissue slice. Yet only those located in pharmacological sanctuaries eventually will be able to outcompete other cell phenotypes.

Both presented protocols resulted in highly heterogeneous tumor with two leading components. Notable is the fact that unlike previous cases, the initial cells of some phenotypes are not from the low-drug normoxic region. For instance, pink triangle phenotype originates from high drug concentration region, but eventually manage to escape in the hypoxic niche being not completely quiescent it continues proliferation until taking over the big part of the domain.

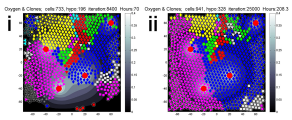

(a) 0.5-0-0.5

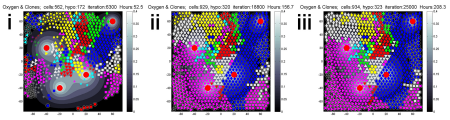

(b) 0.5-0-0.5-0

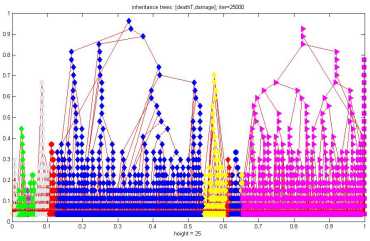

(c) 0.5-0-0.5

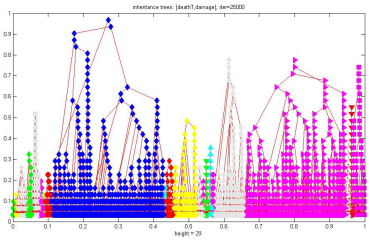

(d) 0.5-0-0.5-0

Figure 4.22: *Clonal evolution*, $increment\_sizes = 5.9 \times 10^{-5}$, $DrugIn = 0.5$ (a),(c) show clonal configuration at the end of drug administrating interval and at the end of the treatment. (b),(d) show phylogenetic trees.

In conclusion, it was shown that dose intensity greatly affect the tumor clonal evolution. Both too low and high doses may trigger tumor heterogeneity which will strongly increase the complexity of the further treatment process. For these cases introducing more fractions will bring more clonal diversity to the tumor, whereas for mid-range drug concentrations more fractions does not necessary contribute to the tumor heterogeneity. Some thoughts about reasonable drug dosage are presented in the next section.

4.3 Drug Response Plots

In this section, the analysis of dose-response curves for the model is presented. Drug-response curves are used in clinical pharmacology to evaluate efficacy and potency of the used drug and define the therapeutic index of the medication. This information is valuable when making a decision on the required drug dose for a patient.
There are quite a variety of choices for response measurements used in experiments investigating drug effects. In this thesis, three types of responses were considered: the amount of killed cells for the efficacy plot; surviving cells to show the inhibition effect; and the time needed to kill all cancer cells to estimate the drug concentration sufficient for complete tumor eradication. The measurements of the mentioned responses are summarized in Table 4.5.
Toxicity in Table 4.5 shows different drug concentrations that will be plotted against the response. Dose-response curves follow the sigmoidal shape, thus the data obtained through the simulations were fitted using a 4 parameter logistic nonlinear regression model [14]: $y = Bottom + (Top - Bottom)/(1 + \left(\frac{x}{Conc_{50}}\right)^{-HillCoeff})$, where Top and Bottom are maximum and minimum response respectively, Hill coefficient determines the slope of the curve and $Conc_{50}$ an inflection point, where the sigmoid curve changes it concavity, shows the drug concentration that induce a half-maximum response. These curves show that at zero or small drug concentrations there is no response to the medication (Bottom), but at some time point increase in drug concentration will trigger the increase in response until a maximum response is reached (Top), which means that increasing drug dose at this point won't benefit the patient but rather give unwanted drug side effects.

increment size 0																	
Toxicity	0	0.25	0.5	0.75	1	1.25	1.5	1.75	2	2.25	2.5	2.75	3	3.25	3.5	3.75	4
Killed Cells till iter 1400	0	0	0	0	0	0	0	33	121	166	178	177	167	164	150	148	141
Survived Cells, iter 8000	915	915	650	9	0	0	0	0	0	0	0	0	0	0	0	0	0
Iterations	8000	8000	8000	8000	6607	4004	3279	2666	2459	2208	1936	1876	1789	1683	1605	1553	1458
increment size 3.5×10^{-5}																	
Toxicity	0	0.25	0.5	0.75	1	1.25	1.5	1.75	2	2.25	2.5	2.75	3	3.25	3.5	3.75	4
Killed Cells till iter 1300	0	0	0	0	0	0	0	0	18	91	149	155	158	159	153	147	145
Survived Cells, iter 25000	930	930	930	936	8	0	0	0	0	0	0	0	0	0	0	0	0
Iterations	25000	25000	25000	25000	25000	7065	3895	3090	2793	2475	2133	2090	2044	1781	1762	1660	1387
increment size 4.5×10^{-5}																	
Toxicity	0	0.25	0.5	0.75	1	1.25	1.5	1.75	2	2.25	2.5	2.75	3	3.25	3.5	3.75	4
Killed Cells till iter 1600	0	0	0	0	0	0	0	45	174	212	208	199	178	167	165	159	155
Survived Cells, iter 25000	930	930	930	930	935	0	0	0	0	0	0	0	0	0	0	0	0
Iterations	25000	25000	25000	25000	25000	8014	4377	3196	3054	2388	2386	2185	2092	1732	1598	1615	1657
increment size 5.9×10^{-5}																	
Toxicity	0	0.25	0.5	0.75	1	1.25	1.5	1.75	2	2.25	2.5	2.75	3	3.25	3.5	3.75	4
Killed Cells till iter 1600	0	0	0	0	0	0	0	11	147	206	219	201	188	173	165	162	160
Survived Cells, iter 25000	930	930	930	930	942	2	0	0	0	0	0	0	0	0	0	0	0
Iterations	25000	25000	25000	25000	25000	25000	5304	3225	2839	2573	2295	2274	1854	1811	1815	1680	1609

Table 4.5: *Drug concentrations and response measurements for different resistance types (no-resistance, acquired resistance).* The amounts of killed and survived cells are computed for fixed treatment time and Iterations show the time needed to eradicate tumor.

Firstly, consider the half-maximal effective concentration EC_{50} of the drug. As the goal of anti-cancer therapy is to kill tumor, the number of killed cells in fixed time interval was considered as a desired drug effect. The number of iterations was fixed for both no-resistance and acquired resistance cases, taking the minimal time needed to eradicate the tumor completely (see Table 4.5 Iterations), thus it is 1400 iterations for no-resistance case, 1300 - for the case with $increment\_sizes = 3.5 \times 10^{-5}$ and 1600 iterations for other cases. Dose-response curves with log of agonist-drug concentration plotted against drug effect are presented in Figure 4.23.

Curves have rather steep slopes with high absolute values of positive Hill coefficients,

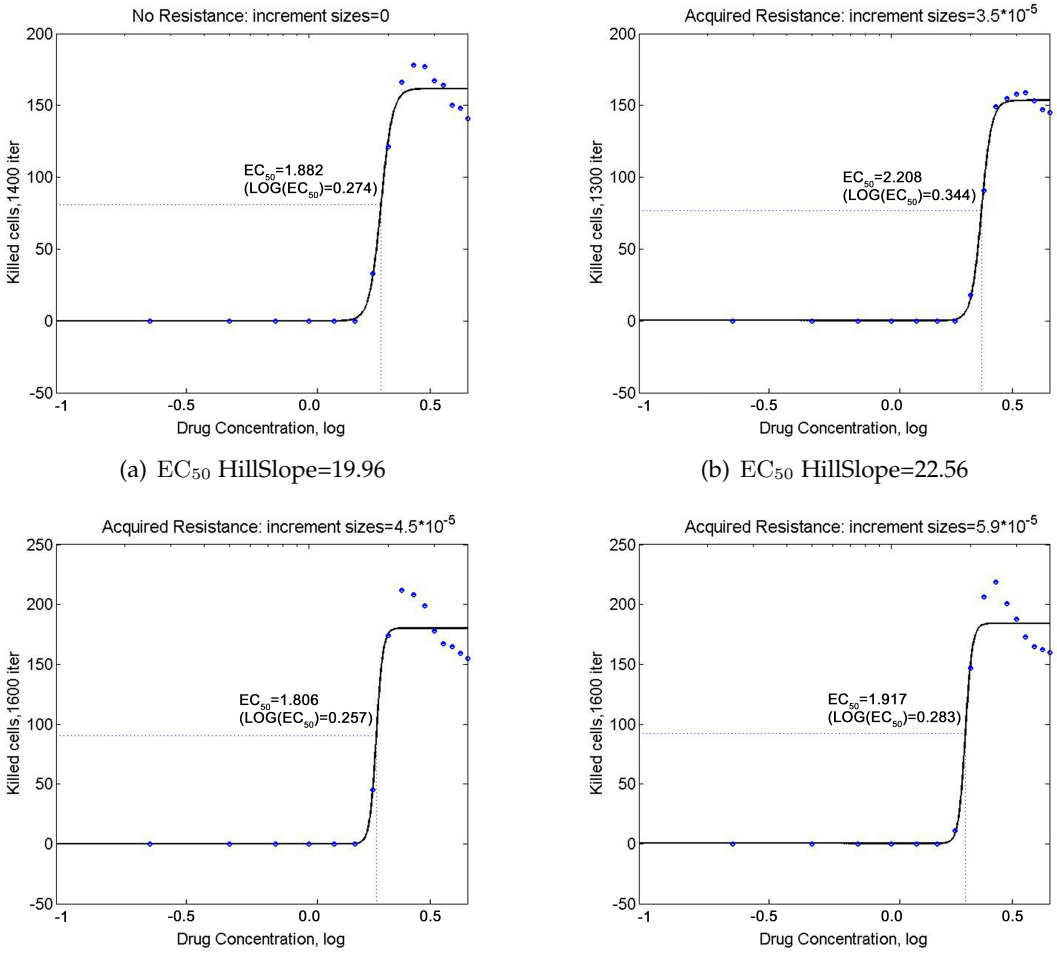

(a) EC_{50} HillSlope=19.96

(b) EC_{50} HillSlope=22.56

(c) EC_{50} HillSlope=34.69

(d) EC_{50} HillSlope=33.42

Figure 4.23: EC_{50} *curves for different resistance types (no-resistance, acquired resistance).* In (a) the no-resistance case is shown, increment sizes = 0. The acquired resistance with increment sizes parameter values 3.5×10^{-5}, 4.5×10^{-5} and 5.9×10^{-5} are shown in (b), (c) and (d) respectively.

curves for acquired resistance are steeper though. Steep slopes mean that it will be quite challenging to determine the right dose to get a particular drug effect without getting side effects. However, this result was something to be expected, as chemotherapeutic drugs are known for their narrow therapeutic window.

The drug potency lies around 2 for all the cases. However, drug is slightly more potent

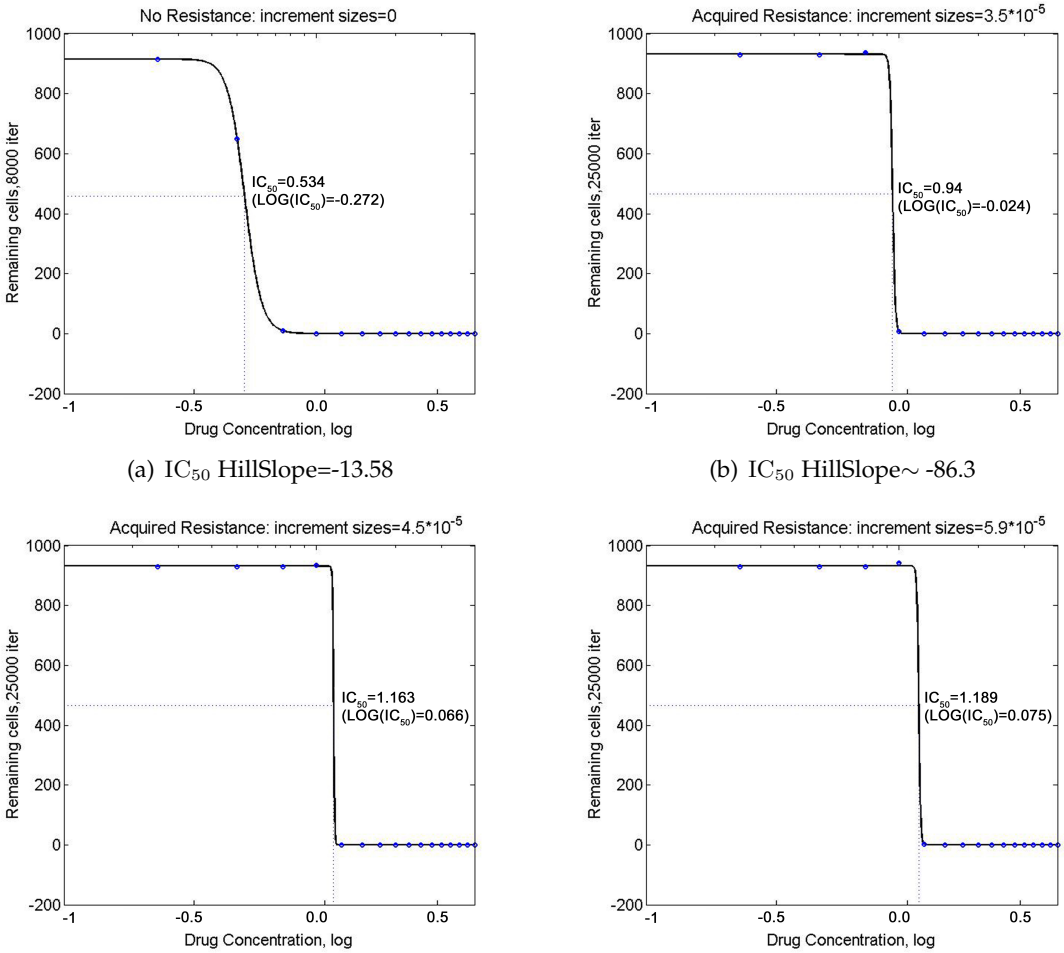

(a) IC_{50} HillSlope=-13.58

(b) IC_{50} HillSlope$\sim$ -86.3

(c) IC_{50} HillSlope$\sim$ -229.8

(d) IC_{50} HillSlope$\sim$ -123.8

Figure 4.24: IC_{50} *curves for different resistance types (no-resistance, acquired resistance).* In (a) the no-resistance case is shown, increment sizes = 0. The acquired resistance with increment sizes parameter values 3.5×10^{-5}, 4.5×10^{-5} and 5.9×10^{-5} are shown in (b),(c) and (d) respectively.

in the case of no-resistance and acquired resistance with $increment\_sizes = 4.5 \times 10^{-5}$, having the lowest EC_{50} values 1.882 and 1.806 respectively. As for the efficacy, the maximum response equals 184 for the case with $increment\_sizes = 5.9 \times 10^{-5}$. Thus for this case the drug was the most efficacious. Quite dispersed response data at the top plateau

can explained with the drug concentration itself. Lower drug concentrations need more time to eradicate tumor, thus there is still plenty of cells at the observed fixed iteration, while for the higher concentrations the tumor is already almost killed off at the observed time point.

Next, the investigation of half-maximum inhibitory drug concentration is provided.

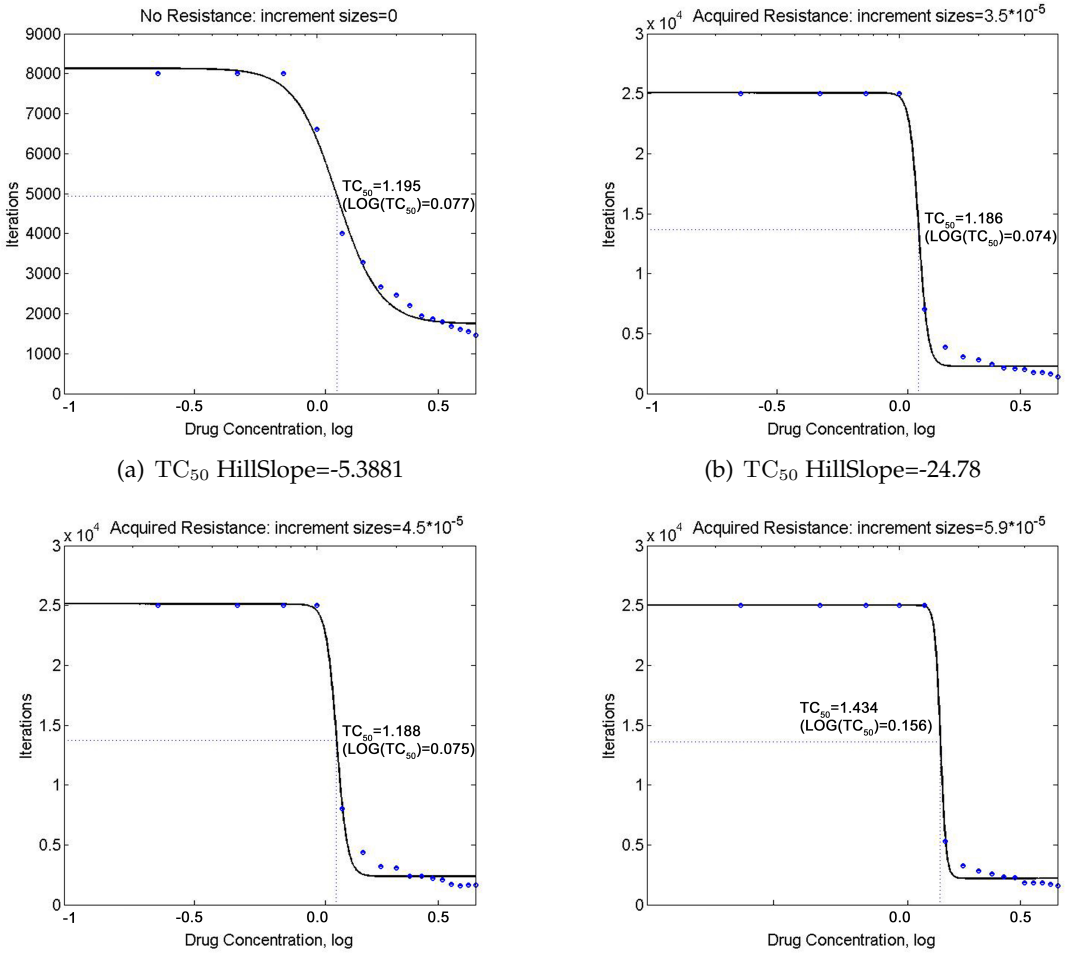

(a) TC_{50} HillSlope=-5.3881

(b) TC_{50} HillSlope=-24.78

(c) TC_{50}HillSlope=-21.36

(d) TC_{50} HillSlope=-40.92

Figure 4.25: TC_{50} *curves for different resistance types (no-resistance, acquired resistance).* In (a) the no-resistance case is shown, increment sizes = 0. The acquired resistance with increment sizes parameter values 3.5×10^{-5}, 4.5×10^{-5} and 5.9×10^{-5} are shown in (b),(c) and (d) respectively.

DNA damaging chemotherapeutic drugs like antimetabolites, alkylating and platinum-based agents, which are considered in this thesis, inhibit the cancer cells growth. Thus, IC_{50} plots are often used as a measure of effectiveness for these types of drugs, where IC_{50} represents the concentration of an anti-cancer drug needed for 50% inhibition.

This time the antagonist-drug concentration is plotted against the inhibition effect, which means a sigmoid has a descending form with negative Hill coefficient Figure 4.24. One can see that the acquired resistance cases have very steep slopes, where Hill coefficients were not estimated well, as a result of Jacobian matrix being ill-conditioned at the solution.
As for the obtained IC_{50} values, they illustrate how the inhibition capacity of the drug is reduced as the cancer cells acquire resistance, the higher the $increment\_sizes$ the higher is IC_{50} value. Thus for the no-resistance case with $IC_{50} = 0.534$ drug is the strongest inhibitor that is active even at low drug dose.
Now, the investigation on the time at which cells are eradicated is presented Figure 4.25. In this case TC_{50} determines the drug concentration at which it takes half of the time to eradicate tumor, comparing to the case with no treatment. The drug appears to be less potent for the case with $incremet\_sizes = 5.9 \times 10^{-5}$ with $TC_{50} = 1.434$. For other cases the drug concentration value at which it take half of the allowed time to eradicate tumor lies around 1.2. The slope fo no-resistance case is somewhat shallow compared to those of acquired resistance, it implies that there are possibility to overlap between desired effects and unwanted side effects of the drug.
In conclusion, as expected, one can see that drug appears to more potent for the no-resistance case, thus allowing to slightly reduce dosage. However, in more realistic setting with cancer that is capable to acquire resistance, especially for high $increment\_sizes$ parameter values, the Hill coefficients have high absolute values, hence, slight changes in drug concentrations may cause unwanted toxic effects. Dose-response curves showed the drug concentrations for half-maximum response, which can help to determine minimal effective dose of the drug. However, to define a pharmaceutical window of observed medication one has to investigate TD_{50} (toxic dose), considering the negative effects drug causes to patient.

5 Discussion

This thesis investigated the impact that the introduction of different drug administration schedules has on the spatial and temporal cancer population dynamics, its clonal diversity and emergence of anti-cancer drug resistance. The analysis was done utilizing a hybrid discrete-continuous mathematical model developed by Gevertz et al. in [9]. To replicate the idea of clinical chemotherapy, drug delivery was modeled by a piecewise constant function that alternates drug administration periods with resting intervals. Tumor behavior under treatment with different chemotherapy regimens for both no-resistance and acquired resistance cases is examined in the thesis.
Several interesting outcomes were obtained through careful analysis of model's numerical simulations: 1). acceptance of no-drug intervals into the treatment schedule, as expected, proved to be beneficial for the patient's condition, through reducing the overall toxicity, however, it also increases time needed for successful tumor eradication; 2). low dose intensity protocols show inferior performance compared to those with high dosages and lead to the tumor heterogeneity; 3). for strongly resistant tumors ($increment\_sizes$ high enough) the effect of particular schedule on the treatment outcome is reduced; 4). dose intensity turned out to have more influence on the therapy result than the number of fractions, which has more impact on the tumor clonal diversity; 5). dose intensity of the first active drug administration interval treatment greatly influences further cancer population behavior; 6). drug concentrations producing half-maximum response correlate with the dose intensities of the optimal protocols.
In clinical practice incorporation of resting intervals in treatment plan is essential as cytotoxicity of DNA damaging chemotherapeutic agents leads to the severe side effects. However, tumor cells repopulation during no-drug periods postpones the cancer cure [20]. All simulations of low drug dose intensity protocols resulted in failed treatment with high clonal diversity of persistent cancer cell population. Negative impact to the treatment outcome of low-dose therapy was observed also in clinical practice [26, 38].
The comparison of acquired resistance cases with different $increment\_sizes$ revealed decreased influence of the particular protocol on the treatment outcome, resulting in tumor expansion over the whole domain. However, the heterogeneity of these remaining cancer populations differs, increasing with intervals number in used regimen. For both resistance types (no-resistance, acquired) the first interval has decided the further disease development, guiding it in a particular direction to vanishing or progression.
It was mentioned before that the obtained results revealed inevitable negative outcome when using low-dose therapy. However, presently more and more medicians choose to lower drug dosage achieving positive treatment results [19]. The reason why the simulations results presented in this thesis haven't benefited cancer defeat is the very objective of metronomic therapy. It observes cancer as chronic disease and is aimed to

maintain it in stable size throughout the patient's lifetime. Metronomic chemotherapy is accompanied by the imunotherapy and inhibition of angiogenesis. Thus, if one was to simulate this treatment approach by means of the model presented in this thesis it would be reasonable to at least change the vasculature geometry to incorporate an extra oxygen deprivation.
Future perspective of research might include simulations of the clinical routine drug administration protocols for particular DNA damaging drugs. The initial cell clones configuration might be adjusted based on patient's histology samples. Incorporation of the normal cells into the model might help to determine the therapeutic window of the modeled drug and further optimize its dosage.

Bibliography

[1] Sudhakar A. History of cancer, ancient and modern treatment methods. 1:1–4, Dec 2009.

[2] Sledge G.W. Allison K.H. Heterogeneity and cancer. 28:772–8, Sep 2014.

[3] Baguley B.C. Multiple drug resistance mechanisms in cancer. 46(3):308–16, Nov 2010.

[4] Nislow C. Cheung-Ong K., Giaever G. Dna-damaging agents in cancer chemotherapy: Serendipity and chemical biology. 20:648–659, May 2013.

[5] Bissell M.J. Correia A.L. The tumor microenvironment is a dominant force in multidrug resistance. 15:39–49, 2012.

[6] Badame R.M. Allen C. Piquette-Miller M. De Souza R., Zahedi P. Chemotherapy dosing schedule influences drug resistance development in ovarian cancer. 10:1289–1299, 2011.

[7] Bates S. Dean M., Fojo T. Tumour stem cells and drug resistance. 5(4):275–284, 2005.

[8] Chu E. DeVita C., Vincent T. A history of cancer chemotherapy. 68, 2008.

[9] Norton K.A. Pérez-Velázquez J. Volkening A. Rejniak K.A. Gevertz J.L., Aminzare Z. Emergence of anti-cancer drug resistance: Exploring the importance of the microenvironmental niche via a spatial model. In A. Radunskaya T. Jackson, editor, *Applications of Dynamical Systems in Biology and Medicine*, pages 1–34. Springer-Verlag New York, 2015.

[10] Maley C.C. Greaves M. Clonal evolution in cancer. 481:306–313, Jan 2012.

[11] Lage H. An overview of cancer multidrug resistance: a still unsolved problem. 65:3145–3167, 2008.

[12] World health organization. Cancer, 2015.

[13] Longley D.B.-Johnston P.G. Holohan C., Van Schaeybroeck S. Cancer drug resistance: an evolving paradigm. 13:714–726, 2013.

[14] Systat Software Inc. Standard curves analysis, 2015.

[15] National Cancer Institute. Cancer screening overview, Jul 2014.

[16] National Cancer Institute. Screening tests, 2015.

[17] Robert J. Comparative study of tumorigenesis and tumor immunity in invertebrates and nonmammalian vertebrates. 34(9):915–925, Sep. 2010.

[18] Liao J.B. Viruses and human cancer. 79(3-4):115–122, Dec 2006.

[19] Klement G.L. Kareva I., Waxman D.J. Metronomic chemotherapy: an attractive alternative to maximum tolerated dose therapy that can activate anti-tumor immunity and minimize therapeutic resistance. 358(2):100–6, 2015.

[20] Tannock I.F. Kim J.J. Repopulation of cancer cells during therapy: an important cause of treatment failure. pages 516–525, Jul 2005.

[21] Levy D. Gottesman M.M. Lavi O., Greene J.M. The role of cell density and intratumoral heterogeneity in multidrug resistance. 73:7168–75, Dec 2013.

[22] Hejmadi M. *Introduction to Cancer Biology*. Ventus Publishing ApS, 2010.

[23] Swanton C. McGranahan N. Biological and therapeutic impact of intratumor heterogeneity in cancer evolution. 27:15–26, Jan 2015.

[24] Loeffler M. Meineke F.A., Potten C.S. Cell migration and organization in the intestinal crypt using a lattice-free model. 34:253–266, 2001.

[25] Polyak K. Michor F. The origins and implications of intratumor heterogeneity. 3:1361–4, Nov 2010.

[26] Cairo M.S. Dose reductions and delays: limitations of myelosuppressive chemotherapy. 14:21–31, Sep 2000.

[27] Division of Cancer Prevention, Centers for Disease Control Control, and Prevention. Breast cancer, 2014.

[28] Division of Cancer Prevention, Centers for Disease Control Control, and Prevention. Cervical cancer, Mar 2014.

[29] Tokimoto C. Page R. *Cancer management: a multidisciplinary approach: medical, surgical, and radiation oncology*. PPR.

[30] Kassen R. Spencer S. Maley C. Pepper J., Findlay C. Cancer research meets evolutionary biology. 2:62–70, 2009.

[31] Corrie P.G. Cytotoxic chemotherapy: clinical aspects. 36, 2008.

[32] Hanahan D. Pietras K. A multitargeted, metronomic, and maximum-tolerated dose "chemo-switch" regimen is antiangiogenic, producing objective responses and survival benefit in a mouse model of cancer. 23(5):939–952, Feb 2005.

[33] Weinberg R.A. *The Biology of Cancer*. Garland Science, 2 edition, 2014.

[34] Papanastassiou V. Rampling R., James A. The present and future management of malignant brain tumours: surgery, radiotherapy, chemotherapy. 75, 2004.

[35] Papac R.J. Origins of cancer therapy. 74:391–398, 2001.

[36] Pajic M. van Leeuwen F.W.B. van der Heijden I. van de Wetering K. Liu X. de Visser K.E. Gilhuijs K.G. van Tellingen O. Schouten J.P. Jonkers J. Borst P. Rottenberg S., Nygren A.O.H. Selective induction of chemotherapy resistance of mammary tumors in a conditional mouse model for hereditary breast cancer. 104:12117–12122, 2007.

[37] Morse H.R. Salehan M.R. Dna damage repair and tolerance: a role in chemotherapeutic drug resistance. 70, 2013.

[38] Rozados V.R. Scharovsky O.G., Mainetti L.E. Metronomic chemotherapy: changing the paradigm that more is better. 16, 2009.

[39] Gilbert S.F. *Developmental Biology*. Sinauer Associates, 6 edition, 2000.

[40] Lang F. Silbernagl S. *Color Atlas of Pathophysiology*. Thieme Verlag, 2 edition, 2009.

[41] Wittekind C. Sobin L.H., Gospodarowicz M.K. *TNM Classification of Malignant Tumours*.

[42] American Cancer Society. Early history of cancer, 2014.

[43] American Cancer Society. Cancer facts and figures 2015, Feb 2015.

[44] American Cancer Society. Testing biopsy and cytology specimens for cancer, Jul 2015.

[45] Patel K. Tannock I.F. Trédan O., Galmarini C.M. Drug resistance and the solid tumor microenvironment. 99:1441–1454, Oct 2007.

[46] Gracova K. Graupera M. Casanovas O. Capellà G. Serrano T. Laquente B. Viñals F. Vives M., Ginestà M.M. Metronomic chemotherapy following the maximum tolerated dose is an effective anti-tumour therapy affecting angiogenesis, tumour dissemination and cancer stem cells. 133(10):2464–72, Nov 2013.

[47] Ndouba A.M. Wandan E.N., Elleingand E.F. A screening for benzo [a] pyrène in cocoa beans subjected to different drying methods during on farm processing. 3(5), 2011.

[48] Turchi J.J. Woods D. Chemotherapy induced dna damage response convergence of drugs and pathways. 14, 2012.

[49] Lambert G. Estévez-Salmerón L. Tlsty T.D. Austine R.H. Sturma J.C. Wu A., Loutherback K. Cell motility and drug gradients in the emergence of resistance to chemotherapy. 110:16103–16108, Oct 2013.

[50] Luqmani Y.A. Mechanisms of drug resistance in cancer chemotherapy. 14:35–48, 2005.

[51] Borden K.L B. Zahreddine H. Mechanisms and insights into drug resistance in cancer, frontiers in pharmacology. 4, 2013.